タイトル	Potential roles of DNA methylation in the initiation and establishment of replicative senescence revealed by array-based methylome and transcriptome analyses
別タイトル	複製老化特異的なDNAメチル化による遺伝子発現の調節
作成者（著者）	榊, みずほ
公開者	東邦大学
発行日	2017.03
掲載情報	東邦大学大学院理学研究科 博士論文.
資料種別	学位論文
内容記述	主査: 永田喜三郎 / 冊子の博士論文にはデータAppendix71-9374pはなし
著者版フラグ	ETD
報告番号	32661甲第855号
学位授与年月日	2017.03.16
学位授与機関	東邦大学
メタデータのＵＲＬ	https://mylibrary.toho-u.ac.jp/webopac/TD17120843

東邦大学審査学位論文（博士）

Potential roles of DNA methylation in the initiation and establishment of replicative senescence revealed by array-based methylome and transcriptome analyses

Mizuho Sakaki

Biomolecular Science Major, Graduate School of Science,
Toho University

2016

CONTENTS

Abstract

Cellular senescence is classified into two groups: replicative and premature senescence. Gene expression and epigenetic changes are reported to differ between these two groups and cell types. Normal human diploid fibroblast TIG-3 cells have often been used in cellular senescence research; however, their epigenetic profiles are still not fully understood. To elucidate how cellular senescence is epigenetically regulated in TIG-3 cells, we analyzed the gene expression and DNA methylation profiles of three types of senescent cells, namely, replicatively senescent, ras-induced senescent (RIS), and non-permissive temperature-induced senescent SVts8 cells, using gene expression and DNA methylation microarrays. The expression of genes involved in the cell cycle and immune response was commonly either down- or up-regulated in the three types of senescent cells, respectively. The altered DNA methylation patterns were observed in replicatively senescent cells, but not in prematurely senescent cells. Interestingly, hypomethylated CpG sites detected on non-CpG island regions ("open sea") were enriched in immune response-related genes that had non-CpG island promoters. The integrated analysis of gene expression and methylation in replicatively senescent cells

demonstrated that differentially expressed 867 genes, including cell cycle- and immune response-related genes, were associated with DNA methylation changes in CpG sites close to the transcription start sites (TSSs). Furthermore, several miRNAs regulated in part through DNA methylation were found to affect the expression of their targeted genes. Taken together, these results indicate that the epigenetic changes of DNA methylation regulate the expression of a certain portion of genes and partly contribute to the introduction and establishment of replicative senescence.

Introduction

Cellular senescence is irreversible cessation of cell proliferation. The phenomenon was first reported by L. Hayflick at 1960's [1, 2]. Cell culture biologists had often observed the limited multiplication of normal human diploid cells *in vitro*. The cause of the limitation had been ascribed to inexperienced culture techniques, insufficiency in media composition and virus contamination. However, L. Hayflick demonstrated that the limitation is not caused by those described above. He hypothesized that the finite lifetime results from chromosome aberrations due to accumulation of DNA damage.

Cellular senescence is classified into two groups: replicative senescence which was found by L. Hayflick and premature senescence [3]. In 1990, C. B. Harley reported telomere shortening in aged cells, the main cause of replicative senescence, which keeps activating DNA damage response (DDR) [4, 5]. On the other hand, premature senescence is caused by stresses such as induction of oncogenic *ras* [6] and reactive oxygen species (ROS) [7] without telomere shortening. These stresses cause continuous DDR as replicative senescence does. Thus continuous activation of DDR

seems to be critical for establishment of cellular senescence. Oncogenic *ras* induced senescence (RIS) has been studied well as a model of premature senescence. In this study, we also investigated the other type of premature senescence using SVts8 cells which are conditionally immortalized cells derived from TIG-3 cells. SVts8 cells harbor a temperature-sensitive (ts) mutant of simian virus 40 large T antigen, and have a high level of endogenous telomerase, thus growing immortally at a permissive temperature (33.5°C), while the cells rapidly fall into an irreversible senescent state at a non-permissive temperature (38°C) [7, 8].

p53, Rb and $p16^{INK4a}$ are well known key factors inducing and maintaining cellular senescence. p53 is activated via DDR pathway through ATM/ATR and CHK1/CHK2 [3, 9, 10]. Activated p53 leads to an increase in p21, and it inhibits cyclin E/Cdk2 complex activity. The inhibition results in binding Rb to E2F, transcriptional factor, by increasing activity of Rb, and then causing cell cycle arrest [9]. However, p53 is not a sole key factor for activating Rb. $p16^{INK4a}$ also inhibits cyclin D and Cdk4, 6 complex, thereby leading to senescence state [9, 11]. Induction of oncogenic *ras* in primary human or mouse cells activates p53 and $p16^{INK4a}$, and causes

permanent G1 arrest [6]. At a permissive temperature, SV40 large T antigen in SVts8 cells keeps the proliferative capacity by blocking both p53 and Rb and by maintaining a high level of telomerase. At a non-permissive temperature, dysfunction of SV40 large T antigen leads to rapid activation of p53 and Rb senescence pathway [7, 8]. In addition, after inducing senescence state, maintenance of the senescence state requires continued activation of both p53 and p16 [11]. Induction and maintenance of the senescence state are regulated by many other effector mechanisms depending on types of stress and cells [10]. By comparing with replicative senescence in TIG-3 cells, RIS and senescent SVts8 cells derived from TIG-3 cells could allow us to delineate the difference between two types of cellular senescence.

Although cellular senescence has been shown to be associated with tumor suppression in several cancers [3, 12, 13], it has been reportedly involved in cancer progression through the induction of epithelial-mesenchymal transitions and tumor invasion [14]. In addition, senescent cells secrete several factors associated with inflammation such as interleukin (IL)-6 and IL-8 [15], which are referred to as senescence-associated secretory phenotypes (SASP). Recently, SASP has

been implicated in the pathogenesis of age-related diseases such as rheumatoid arthritis, periodontitis and Alzheimer's disease [14, 16]. Therefore, elucidation of the mechanism contributing to induction and establishment of the senescence state will help overcome such age-related diseases.

Epigenetic regulation such as histone modification, DNA methylation and interference with micro RNA (miRNA) is one of the mechanisms that modulates gene expression.

The tail domain of histone is modified post-transcriptionally by acetylation, methylation, ubiquitination and others, which are called histone modification. The histone modifications alter histone structure, and influences transcription activity positively or negatively, depending on types of modification [17]. Alteration of the chromatin structure occurs in human senescent fibroblasts, where epigenetic regulation contributes to the establishment of the senescent state partly through the $p16^{INK4A}$ / retinoblastoma (RB) protein pathway [18]. Modification of histones, trimethylated histone H3 at lysine9 (H3K9me3) and trimethylated histone

H3 at lysine 27 (H3K27me3) is enriched in the senescence-associated heterochromatic foci (SAHF), although spreading of repressive histone marks is not necessary for SAHF formation [19]. So far as known, histone modification is reportedly involved in expression of key molecules of senescence, such as $p16^{INK4A}$, $p14^{ARF}$ and p53. Loss of H3K27me3 is involved in expression of $p16^{INK4A}$ and $p14^{ARF}$, whereas H4 acetylation and trimethylation of histone H3 at lysine 4 (H3K4me3) are involved in expression of p53 [20-23]. Furthermore, A. Takahashi *et al.* [24] showed that the expression levels of SASP factors, IL-6 and IL-8, are regulated by demethylation of H3K9 through the APC/C^{Cdh1}-G9a/GLP pathway.

5' cytosine residue of DNA is post-transcriptionally methylated by DNA methyltransferase [25, 26]. About 40% of promoter and exon regions comprise CpG islands, which is generally unmethylated [27]. DNA methylation at CpG islands relates to gene transcriptional repression [26, 28]. DNA methylation changes have also been observed during cellular senescence and individual aging. Many studies have elucidated the role of epigenetics in senescence using various approaches such as pyrosequencing, array-based methylome and combined bisulfite restriction analysis (COBRA),

as well as using various types of cells and different tissues derived from genetically different individuals [29-32]. These studies have shown that DNA methylation profiles are tissue- and cell-type specific, and the epigenetic control of gene expression seems to promote in part tissue- and cell-type specific differentiation in addition to cellular senescence. For instance, the DNA methylation profile of fibroblast cells is different from that of mesenchymal stromal cells [33]. Moreover, principal component analysis showed that the methylation pattern of fibroblast cells from one dermal region is different from that from other dermal regions [34]. Christensen *et al.* also showed interindividual variation in methylation profiles among 11 tissues, including blood and brain [35]. In contrast to the studies using genetically different tissues and cells derived from individuals, age-related changes in DNA methylation between monozygotic twins were reported to arise with chronological time, indicating that the differences in genetically identical individuals are driven by different cellular responses to environmental changes [36]. Therefore, we hypothesized that a specific type of cultured cell leading to senescence states induced by different methods and demonstrating differences in methylation profiles will allow us to

characterize in detail the role of epigenetic regulation in response to cellular senescence.

The effects of DNA methylation on gene transcription have been extensively studied in relation to the states of CpG islands (CGIs) near the transcription start sites (TSS). According to recent studies examining the relationship between gene body methylation and gene expression, hypermethylation correlated to not only high gene expression but also low gene expression [37], suggesting a more complex regulation. Varley *et. al.* also reported that the relationship between methylation and gene expression is context-dependent, although the current models reported by several groups indicate that methylation in the promoter regions is associated with gene silencing, and gene body methylation is associated with expression [31].

miRNA is one of the non-coding RNA. It is non-protein-coding single-stranded small RNAs consisting of approximately 18 to 25 nucleotides. The main function of miRNA is negative regulation of gene expression by binding to messenger RNA (mRNA)[38, 39]. Some senescence-associated genes are regulated in part by miRNA [40-44]. miR-34 has been well known as a tumor suppressor and its targeted genes encode the cell cycle regulators

including E2F, c-Myc, cyclin D1, cyclin E2, cdk4, and cdk6 [45-47]. Recent studies on cancers have revealed that the expression of some tumor suppressive miRNAs is regulated by DNA methylation in the miRNA promoter regions [48-50]. Despite these recent advances, much of the relationship between DNA methylation and miRNA expression and how this relates to senescence genes remains unclear.

In this study, we examined characteristic features of DNA methylation during cellular senescence using TIG-3 cells established from fetal lung fibroblasts. Although such TIG-3 cells have been a common focus in senescence research, much of the epigenetics remains unexplored. To test the hypothesis that the differences in genetically identical cells are driven by different cellular responses to senescence, we examined array-based gene expression and DNA methylation profiles using genetically identical TIG-3 cells which had been induced to a senescent state by three different methods, namely, replicatively senescent, *ras*-induced senescent (RIS), and senescent SVts8 cells. We then searched for the positional trend of methylation changes and the possible effects of DNA methylation changes on gene

expression using integrated analysis.

Materials and Methods

Cells and cell culture

Normal human diploid fibroblast TIG-3 cells (obtained from the Health Science Research Resources Bank, Japan) were cultured in DMEM+GlutaMAX-I (GIBCO) supplemented with 10% fetal bovine serum (FBS) (HyClone) and 1% penicillin/streptomycin (Nacalai Tesque) at 37°C under a 5% CO_2 atmosphere. TIG-3 cells were cultured until they senesced at population doubling level (PDL) 85. The TIG-3 cells were harvested for DNA extraction at PDL 36, 49, 69 and 85, for RNA extraction to analyze gene expression at PDL 36 and 84, and for RNA extraction to analyze miRNA expression at PDL 44, 60, 78 and 80.

To prepare RIS cells, retroviral infection was performed as reported previously [51]. Briefly, Phoenix-Eco cells (obtained from Dr. G. P. Nolan, Stanford University, CA, USA) were transfected with the pBabe-puro-H-Ras-V12 or pBabe-puro plasmid by the Chen-Okayama method [52]. Viral supernatants were prepared from the cells after transfection, passed through a 0.45-μm-pore-size syringe filter, and pooled. The supernatant and 8 μg/mL hexadimethrine bromide (Sigma-Aldrich) were

added to TIG-3 cells expressing an ecotropic receptor at a proliferating phase. After infection, the cells were selected with growth medium containing 300 μg/mL G418 and 2 μg/mL puromycin for 9 days before being harvested.

SVts8 cells (obtained from the Health Science Research Resources Bank, Japan) [8] continued to proliferate at a permissive temperature (33.5°C), because of suppression of RB and p53 through induction of a temperature-sensitive mutant of the simian virus (SV) 40 large T antigen to TIG-3 cells and the high ability of telomere maintenance. Senescent SVts8 cells were obtained by culturing SVts8 cells at a non-permissive temperature (38°C) for 6 days.

Microarray assays

Gene expression

Total RNA was isolated with a ReliaPrep RNA Cell MiniPrep System (Promega) according to the manufacturer's instructions. Starting with 200 ng of the isolated RNA for each sample, double stranded cDNA and cyanine 3 labeled cRNA were synthesized using a low input quick amp labeling kit (one-color) and RNA spike-in kit (Agilent). The labeled cRNA was purified

with an RNeasy mini kit (Qiagen), and hybridized to a SurePrint G3 Human GE microarray 8×60K Ver. 2.0 (Agilent). After washing the microarray to remove unhybridized cRNA, the microarray was scanned with an Agilent DNA microarray scanner G2505B, and then feature extraction was performed using the GE1_QCMT_Sep09 protocol.

DNA Methylation

Genomic DNA was isolated using DNeasy Blood & Tissue (Qiagen) according to the manufacturer's instructions. Genomic DNA (1.5 μg) was bisulfite-converted using the EpiTec Plus DNA Bisulfite Kit (Qiagen). From each sample, 300 ng of bisulfite-treated DNA was subjected to DNA methylation profiling using an Infinium HumanMethylation27 or HumanMethylation450 BeadChip array (Illumina) according to the manufacturer's standard protocol. The array slides were scanned with an iScan system (Illumina).

MicroRNA (miRNA) expression

Total RNA including miRNA was isolated with a ReliaPrep miRNA Cell and

Tissue MiniPrep System (Promega) according to the manufacturer's instructions. Approximately 100 ng of the isolated RNA for each sample was labeled with cyanine 3 using miRNA Complete Labelling and Hyb Kit (Agilent) according to the manufacturer's protocols. The labeled RNA was hybridized to a SurePrint G3 Human miRNA Microarray (Release 21.0) (Agilent). After washing, the microarray was immediately scanned using one color scan setting for 8×60k array slides with an Agilent DNA microarray scanner G2505C. The images were extracted with Feature Extraction Software 10.7.3.1 (Agilent) using default parameters.

Data analysis

Gene expression

The SurePrint G3 Human GE microarray data were analyzed using the Subio Platform (Ver. 1.18.4625). The data were normalized as to low signal cutoff (cutoff 1.0 and replace), log transformation (base 2), and global normalization (percentile 75), and then the ratios to those of the control sample (mean) were obtained. In this study, >= 2-fold and =< 0.5-fold changes were regarded as up- and down-regulated gene expression,

respectively. In order to calculate fold-change differences and construct a heatmap, each gene expression level in the senescent cells was compared with that in the control cells, namely replicative senescent cells versus proliferating cells, RIS cells versus cells infected with the empty vector, and senescent SVts8 cells versus proliferating SVts8 cells. The heatmap with sample clustering was drawn using Subio Platform with Uncentered Correlation. The microarray data for gene expression have been deposited in the GEO (GSE81798).

DNA Methylation

The Infinium HumanMethylation27 BeadChip includes probes for 27,578 CpG sites [53]. The Infinium HumanMethylation450 BeadChip includes probes for 485,577 CpG sites covering 21,231 RefSeq genes (99%), and 26,658 CGIs (96%), and 3,091 probes for non-CpG loci [54]. The image data obtained by the iScan system were subjected to background subtraction and control normalization using GenomeStudio V2011.1 (Illumina). Methylation levels were calculated as β values (= intensity of the methylation allele / [intensity of the unmethylated allele + intensity of the methylated allele +100]), which

ranged from 0 (0% methylation) to 1 (100% methylation). Probes for CpG sites with a detection p-value of > 0.05 or a blank ß value were eliminated from further analysis. The ß values of control cells were subtracted from those of senescent cells (Δß). Δß >= 0.2 and Δß =< −0.2 were regarded as hyper- and hypomethylation in this study. TIG-3 cells at PDL 36 were regarded as control cells for those at higher PDLs (49, 69, and 85). An Infinium HumanMethylation27 BeadChip was used to obtain methylation profiles for all samples (TIG-3, RIS, and SVts8 cells). An Infinium HumanMethylation450 BeadChip was used to obtain more comprehensive methylation profiles of TIG-3 cells at PDL 36 and PDL 85, and RIS cells. The BeadChip data have been deposited in the GEO (GSE81788 and GSE81797). Scatter plots for ß values were drawn using Genome Studio. Hyper- and hypo-methylated CpG sites were classified into six CpG subcategories depending on the location relative to the CpG island (CpG island, N_Shore, S_Shore, N_Shelf, S_Shelf, and the open sea) and into seven gene feature subcategories (− 1500 to − 200 bp upstream of the TSS (TSS1500), − 200 bp to 0 bp upstream of TSS (TSS200), 5' untranslated region (5'UTR), first exon (1st exon), gene body, 3' untranslated region (3'UTR), and intergenic region),

according to the probe annotation (HumanMethylation450_15017482_v.1.1.csv) provided by Illumina [55].

Integrated analysis of DNA methylation and gene expression

Normalized gene expression and DNA methylation array data were integrated based on the genomic locations of the RefSeq genes' TSS composed in the expression array and the genomic location of the CpG sites placed in the BeadChip array using custom perl scripts. RefSeq information was retrieved from http://hgdownload.cse.ucsc.edu/goldenPath/hg19/database/refGene.txt.gz. We assessed Δβ values for the CpG sites located within 8 kb distance from the closest TSS of the RefSeq genes and the fold-change value of the corresponding gene expression. The gene expression data were obtained from probes annotated by the RefSeq ID for mRNA. When multiple expression probes existed in the same RefSeq ID, the mean of multiple intensities was calculated for the RefSeq ID. The distance from the methylation site to the TSS was calculated with a computer using the location information on the methylation probes and RefSeq (as described above). Promoters registered in

RefSeq were classified into two classes, CGI and non-CGI promoters, using the following criteria: >= 50% GC content and observed-to-expected ratio of CpG >= 0.6.

Gene ontology (GO) analysis

GO analysis was performed using the Database for Annotation, Visualization and Integrated Discovery (DAVID) v6.7 (http://david.abcc.ncifcrf.gov/) [15-17] with GOTERM_BP_ALL and functional annotation clustering. The genes for GO analysis were extracted according to each cut-off value given in the methylation and integrated analysis section. For GO analysis using only gene expression data, genes exhibiting a more than 3-fold change of expression were used due to the limited gene numbers loaded onto the annotation tool. The top 10 represented GO terms are shown in Table 2, and S1 and S2 Tables. Enrichment scores of more than 1.3 gave p-values of less than 0.05.

To conduct GO analysis on gene feature- and CpG site-categories, the genes related to differentially methylated CpG sites on the gene-coding region based on the probe annotation were analyzed with GOTERM_BP_ALL and a

functional annotation chart due to the small numbers of extracted genes. The ratios of the number of genes with similar functions were calculated for all gene feature- and CpG site-subcategories (Figs. 5 and 6, and S3 Table).

miRNA expression regulated by DNA methylation and its targeted genes

To measure the expression level of miRNAs during replicative senescence, the Human miRNA microarray data were analyzed using GeneSpring (Ver. 12.5). The data were normalized by a 90-percentile shift, and then the ratios to those of the control sample (PDL 44) were obtained. The cut-off for miRNA expression change used in this study was a ±1.5-fold change. The microarray data for miRNA expression have been deposited in the GEO (GSE90942). miRNAs exhibiting methylation changes were obtained from HumanMethylation450 BeadChip data using the "MIR" keyword in the "UCSC_REFGENE_NAME" column provided by Illumina. We searched for miRNAs with hypermethylated promoter regions and down-regulated expression, and vice versa, by comparing methylation changes (Δβ cut-off was ±0.2) with expression changes (fold-change cut-off, ±1.5). Genes targeted

by those miRNAs for which expression seemed to be regulated by DNA methylation were picked up by TargetScanHuman Release 7.0. The resulting genes were then further filtered by more than two miRNAs and the gene expression levels based on our microarray data.

Results

Similar biological outcomes, but different gene expression patterns were detected in three types of senescent cells

We prepared three types of senescent cells, namely, replicatively senescent, RIS and senescent SVts8 cells. The senescence state in SVts8 cells was rapidly induced by the inactivation of the temperature-sensitive mutant of the SV40 large T antigen under non-permissive temperature. Senescence was confirmed by the growth arrest, appearance (a large flat morphology), senescence-associated beta-galactosidase (SA-β-Gal) activity, and protein and mRNA levels of $p16^{INK4A}$ and $p21^{Cip1/Waf1}$ (S1 Fig). Gene expression data for senescent cells obtained with SurePrint G3 Human GE microarrays (Agilent) showed that less than 10% of the probes tended to show similar changes in the three types of senescent cells (up-regulated: 358 of 4,355 probes in replicatively senescent cells, 3,927 probes in RIS cells and 5,124 probes in senescent SVts8 cells; down-regulated: 278 of 4,679 probes in replicatively senescent cells, 4,557 probes in RIS cells and 3,823 probes in senescent SVts8 cells), whereas more than 50% of the probes showed changes specific to each type of senescent cell (up-regulated: 2,396 of 4,355

probes in replicatively senescent cells, 2,384 of 3,927 probes in RIS cells, and 3,408 of 5,124 probes in senescent SVts8 cells; down-regulated: 2,561 of 4,679 probes in replicatively senescent cells, 2,750 of 4,557 probes in RIS cells, and 2,840 of 3,823 probes in senescent SVts8 cells) (Fig. 1). A heatmap also showed different patterns of gene expression among the three types of senescent cells, even though sample clustering indicated that replicatively senescent cells and RIS cells were closer than senescent SVts8 cells (Fig. 2).

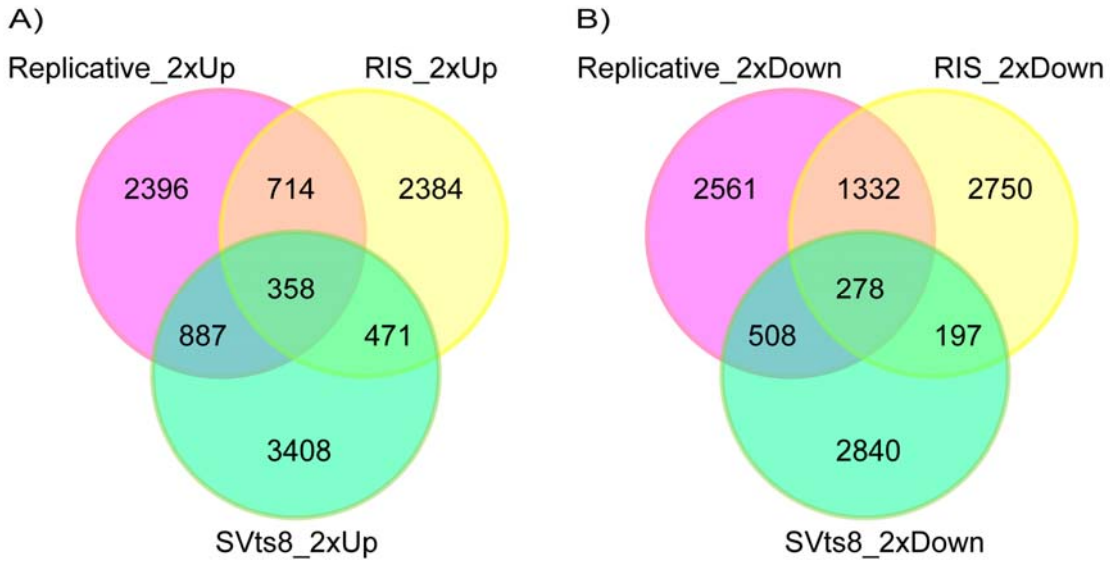

Fig. 1. The number of probes indicating up- or down-regulated genes in three types of senescent cells.

The number of up-regulated (A) or down-regulated probes (B) are shown in three types of senescent cells. The probes exhibiting a more than 2-fold change were counted.

Purple circles, replicatively senescent cells; yellow circles, RIS cells; green circles, senescent SVts8 cells.

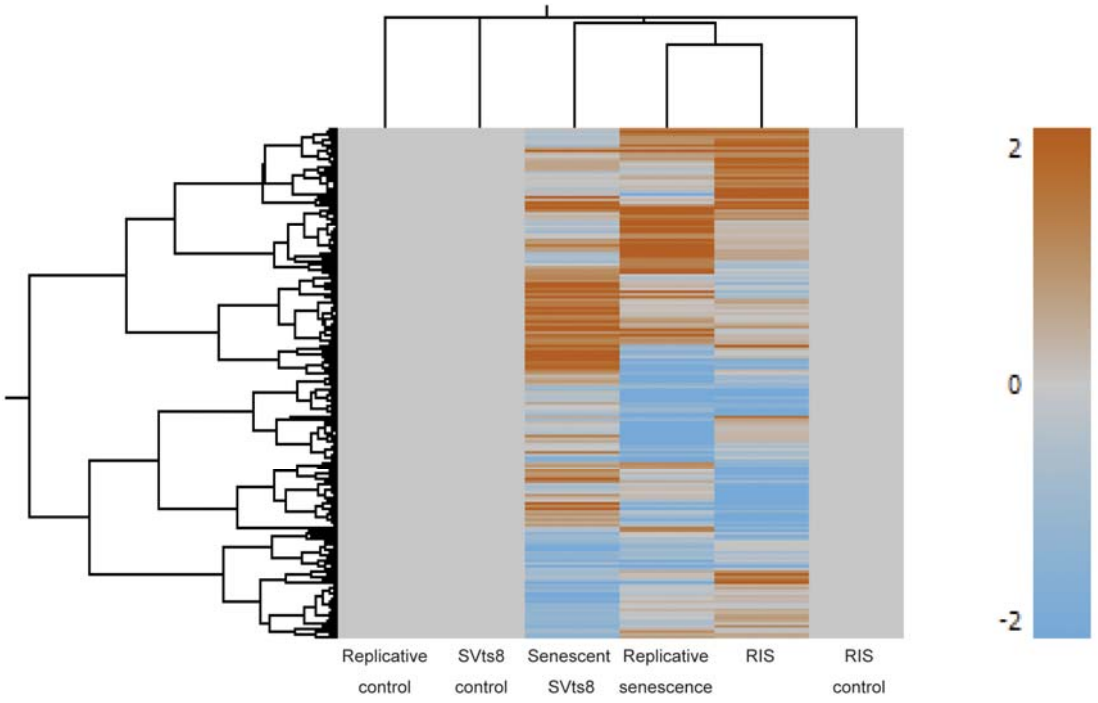

Fig 2. Heatmap of gene expression in three types of senescent cells.

Gene expression patterns in three types of senescent cells are shown as a heatmap with sample clustering using uncentered correlation.

According to the GO analysis of more than 3-fold changed genes, the down-regulated genes in the replicatively senescent, RIS and senescent SVts8 cells were mostly related to the "cell cycle" (S1 Table). On the other hand, the up-regulated genes were related to "immune response",

"locomotion", and "cell migration" in all three types of senescent cells that we examined. Both up-regulated and down-regulated genes included "developmental process" genes. The results suggest that different genes with similar functions contributed to the senescent process, although the biological outcomes were similar among the three types of senescent cells.

Replicatively senescent cells showed DNA methylation changes

The DNA methylation profiles of senescent and proliferating cells were obtained using the Infinium HumanMethylation27 BeadChip. Among the three types of senescent cells examined, only the replicatively senescent cells (TIG-3 at PDL 85) were notably differentially methylated compared to the proliferating control cells (TIG-3 at PDL 36), whereas prematurely senescent cells (RIS and SVts8) were not (Fig. 3, upper panels). Among the 629 and 366 CpG sites that were hyper- and hypo-methylated, respectively, in TIG-3 at PDL 85 (Fig. 3, lower table), 565 (89.8%) and 310 (84.7%) sites showed a stepwise increase and decrease, respectively, of DNA methylation along with the progression of PDLs (36, 49, 69, and 85) (Table 1). Genes hosting the

differentially methylated CpG sites detected in TIG-3 at PDL 85 were subjected to GO analysis using DAVID. Genes associated with hypomethylated CpG sites were found to be most enriched in the term "immune response" (enrichment score 7.86) and its related terms (S2 Table). On the other hand, genes associated with hypermethylated CpG sites were enriched in a wider variety of terms such as regulation of biological and developmental processes with lower enrichment scores (4.24 or lower).

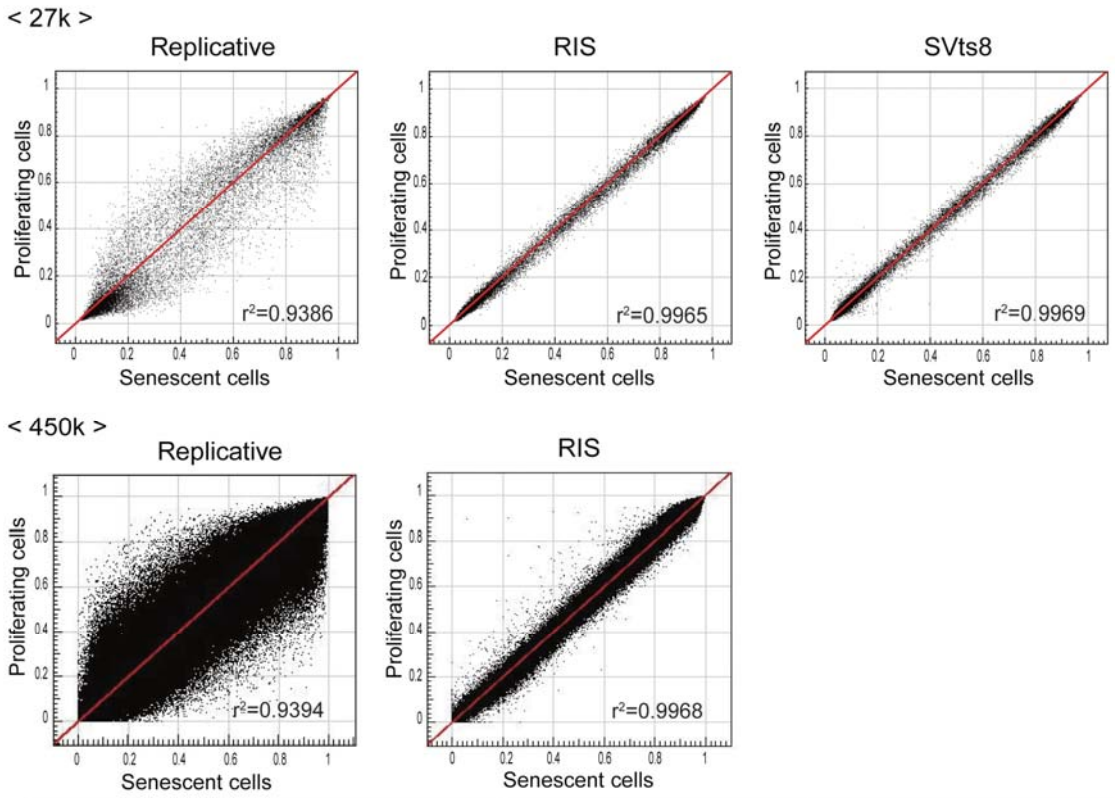

BeadChip type	Total probe number	Replicative senescence		RIS		Senescent SVts8	
		Changed probe number and ratio		Changed probe number and ratio		Changed probe number and ratio	
		Hypo	Hyper	Hypo	Hyper	Hypo	Hyper
27k	27567	366 (1.328%)	629 (2.282%)	0 (0.000%)	0 (0.000%)	2 (0.007%)	1 (0.004%)
450k	484662	12727 (2.626%)	14214 (2.933%)	67 (0.014%)	6 (0.001%)	NA	NA

Fig. 3. Comparison of DNA methylation profiles in three types of senescent cells.

DNA methylation ß values of senescent (x-axis) and proliferating control (y-axis) cells in the three types of senescent models are shown in scatter plots. The data were obtained by Infinium HumanMethylation27 (upper panels, A–C) and HumanMethylation450 BeadChip (middle panels, D–E). The correlation coefficient (r^2) is shown in each plot. The lower table (F) shows the numbers of CpG sites that were hyper- ($\Delta\beta >= 0.2$) and hypo-methylated ($\Delta\beta =< -0.2$) upon senescence.

Table 1. Sequential changes of DNA methylation during replicative senescence.

		PDL 49 vs PDL 36	PDL 69 vs PDL 36	PDL 85 vs PDL 36
Hypomethylated CpG sites	Total number	64	165	366
	Number of sites with sequential change	—	156 (94.5%)	310(84.7%)
Hypermethylated CpG sites	Total number	76	277	629
	Number of sites with sequential change	—	273 (98.6%)	565 (89.8%)

To more comprehensively examine the alteration of DNA methylation upon senescence, we obtained the DNA methylation profiles of TIG-3 cells at PDL 36 and PDL 85, and RIS cells using the Infinium HumanMethylation450 BeadChip. Again, replicatively senescent TIG-3 cells were differentially methylated compared to the proliferating control cells, whereas RIS cells were not (Fig 3D and E). Among 484,662 probes that passed quality control procedures, 14,214 and 12,727 probes were hyper- and hypo-methylated, respectively, in TIG-3 cells at PDL 85 as compared with TIG-3 cells at PDL 36 (Fig. 3F). The ratios of differentially methylated probes were determined for each of the seven gene features and six CpG subcategories (Fig. 4). The frequency of hypermethylated CpG sites was higher than that of hypomethylated CpG sites in TSS1500 (1.6 fold), TSS200 (2.1 fold), 5'UTR (1.5 fold), 1st exon (2.0 fold) and gene body (1.2 fold) subcategories (Fig. 4A).

As shown in Fig. 4B, the frequency of hypermethylated CpG sites was higher in CGI (16.0 fold), N_Shore (2.2 fold), and S_shore (2.4 fold) subcategories, but was lower in N_Shelf (0.44 fold), S_Shelf (0.39 fold), and the open sea (0.51 fold) subcategories. We applied GO analyses to genes hosting the differentially methylated CpG sites to characterize the features of the genes that were supposed to be regulated in part by DNA methylation in each gene feature- and CpG site-subcategories. A total of 8,114 genes hosting the differentially methylated CpG sites were classified by GO terms into the subcategories. The GO terms obtained from functional annotation charts using DAVID were further categorized into seven groups: "immune response", "metabolic process", "transport", "cell adhesion", "development", "signal transduction", and "transcription", plus an additional group, others (Figs. 5A–H and 6A–H, and S3 Table). The "immune response"-related genes hosting hypomethylated CpG sites were enriched in all of the gene feature subcategories, whereas a small portion of those hosting hypermethylated sites were located in the TSS1500, 5'UTR, 1st exon and gene body subcategories (Fig. 5A). Interestingly, in the region from − 200 bp to 0 bp upstream of TSS (TSS200), all of the classified 63 genes related to "immune

response" consisted of the hypomethylated CpG sites. Consistent with the results of GO analyses using HumanMethylation27 data (S2 Table), the genes hosting hypomethylated CpG sites were found to be markedly enriched with the genes involved in "immune response". In sharp contrast, the "transcription"-related genes hosting hypermethylated CpG sites were enriched in all of the gene feature subcategories except for "1st exon", whereas no "transcription"-related genes hosting the hypomethylated ones were located in the gene feature subcategories except "gene body" (Fig. 5G). The results of the GO analyses conducted on the CpG site subcategories are shown in Fig. 6. Genes related to "immune response" were enriched only in the genes hosting hypomethylated CpG sites in the "open sea", but not those in other subcategories (islands, shores, and shelves) (Fig. 6A). In addition, genes related to "transcript" were enriched in the genes hosting hypomethylated CpG sites in the "CpG islands" (Fig. 6G). However, genes related to the other six groups of GO terms were enriched in the genes hosting hypomethylated CpGs in several CpG subcategories (Fig. 6B–F and H). When we focused on the genes hosting hypermethylated CpG sites, genes related to "immune response" were enriched in "N_shore" rather than in the

"open sea". In addition, genes related to other groups were enriched in the genes hosting hypermethlated CpG sites regardless of the CpG site locations (islands, shores, shelves, and the open sea) (Fig. 6B–G). Thus, a certain portion of "immune response"-related genes might be regulated in part by DNA methylation via CpG sites being outside of the CpG islands.

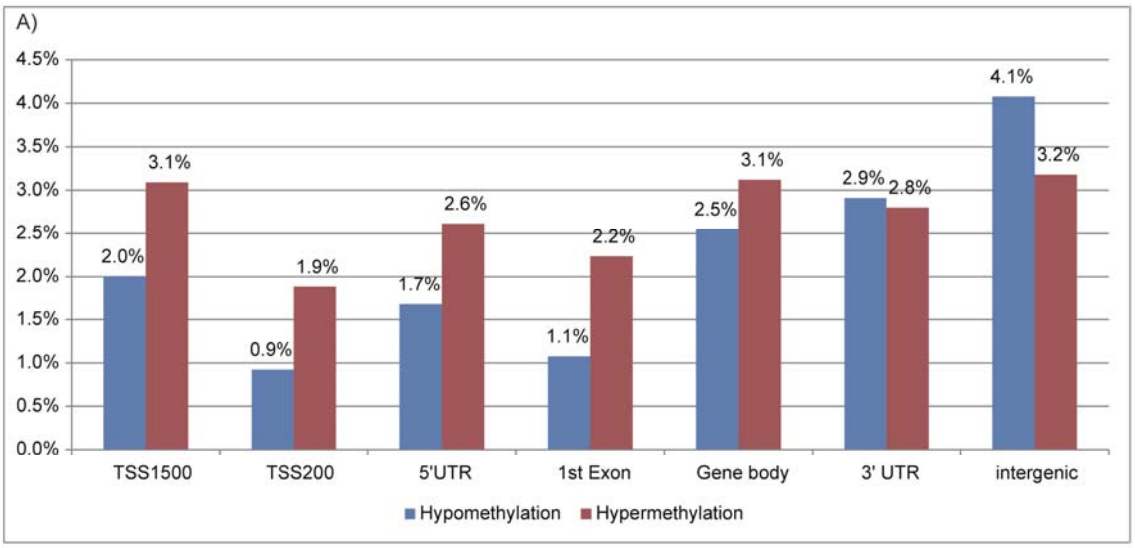

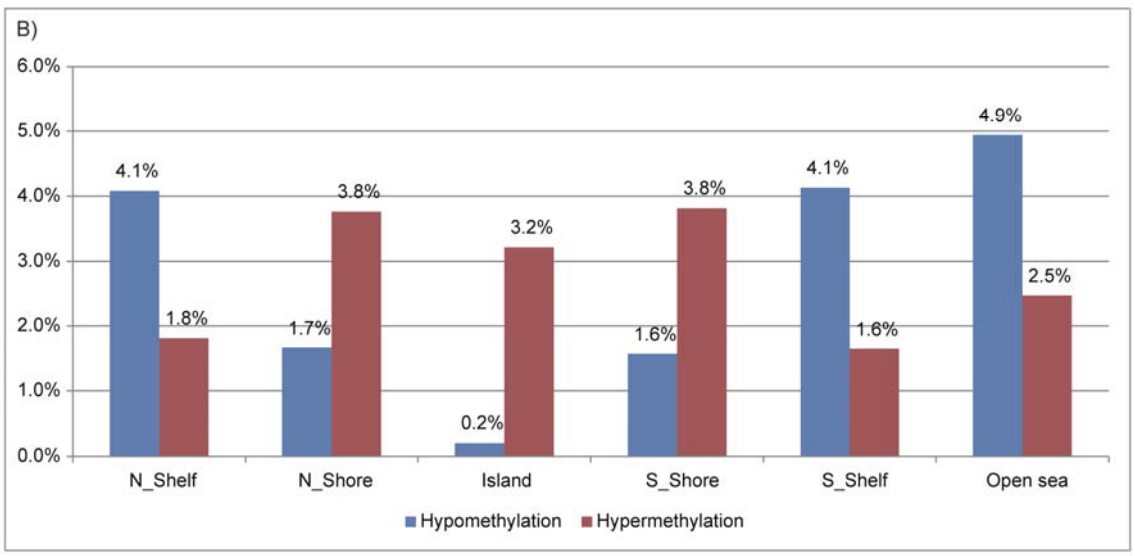

Fig. 4. Rates of differentially methylated CpG sites in replicatively senescent TIG-3 cells in seven gene- feature (A) and six CpG- site (B) subcategories.

CpG sites showing Δβ >= 0.2 and Δβ =< −0.2 in senescent TIG-3 cells (at PDL 85) compared to those at PDL 36 were regarded as hyper- and hypo-methylated, respectively. Seven gene-feature subcategories: TSS1500, TSS200, 5'UTR, 1st exon, gene body, 3'UTR, and intergenic region. Six CpG subcategories: CpG island, N_Shore, S_Shore, N_Shelf, S_Shelf, and the open sea.

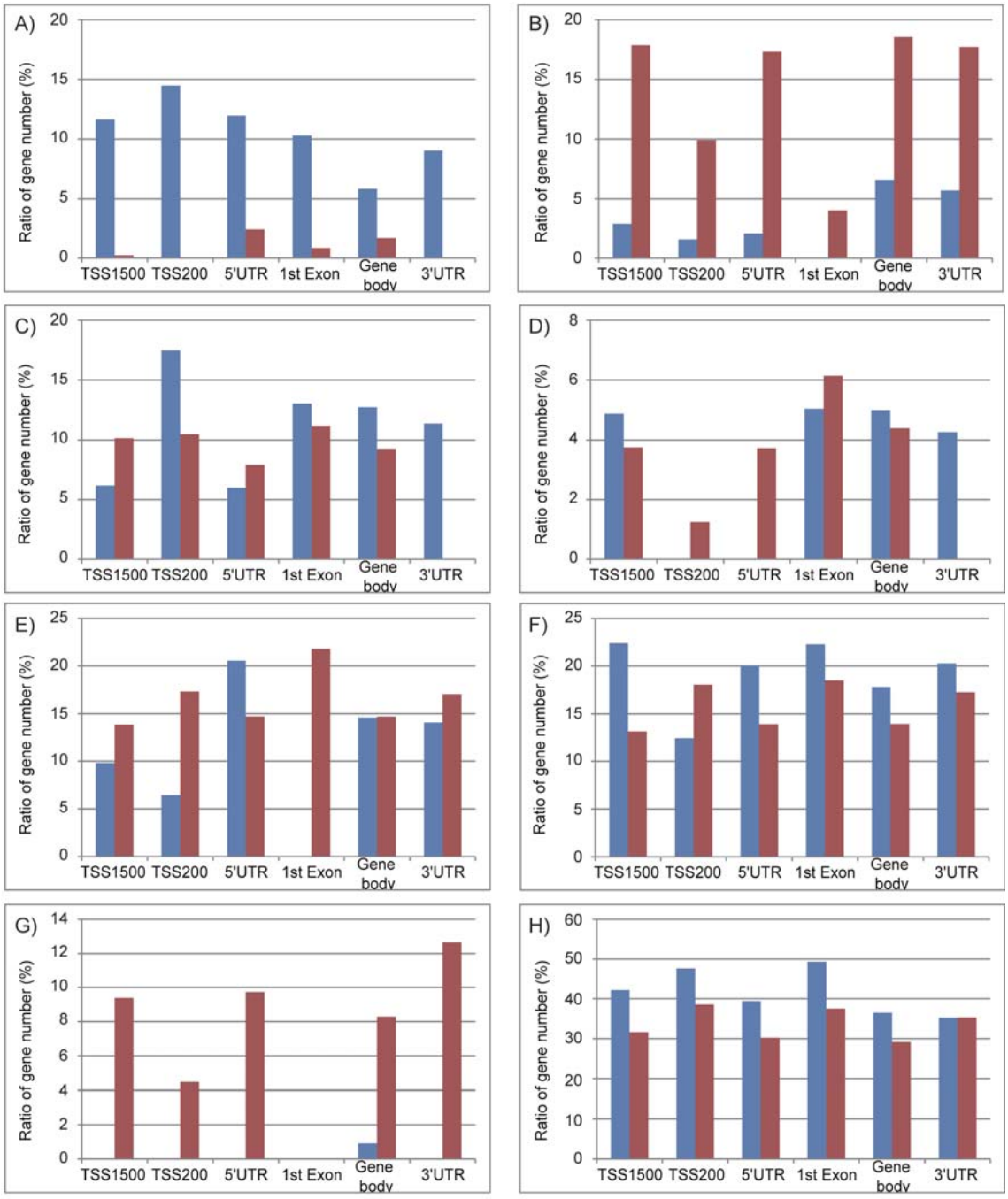

Fig. 5. The characterization of genes hosting differentially methylated CpG sites in the gene feature subcategories.

GO analyses for gene hosting differentially methylated CpG sites were performed using DAVID (functional annotation chart and GOTERM_BP_ALL). The genes hosting

hypermethylated (red) or hypomethylated (blue) CpG sites were classified into six gene feature categories (TSS1500, TSS200, 5'UTR, 1st exon, gene body and 3'UTR). Using the GO terms detected to be enriched (p-value =< 0.05) by DAVID, genes with similar functions were classified into seven groups: immune response (A), metabolic process (B), transport (C), cell adhesion (D), development (E), signal transduction (F), and transcription (G), plus an additional group, others (H). Histograms (A–H) show the ratio of the number of genes classified by GO terms in gene features subcategories (S3 Table shows the number of genes analyzed and classified).

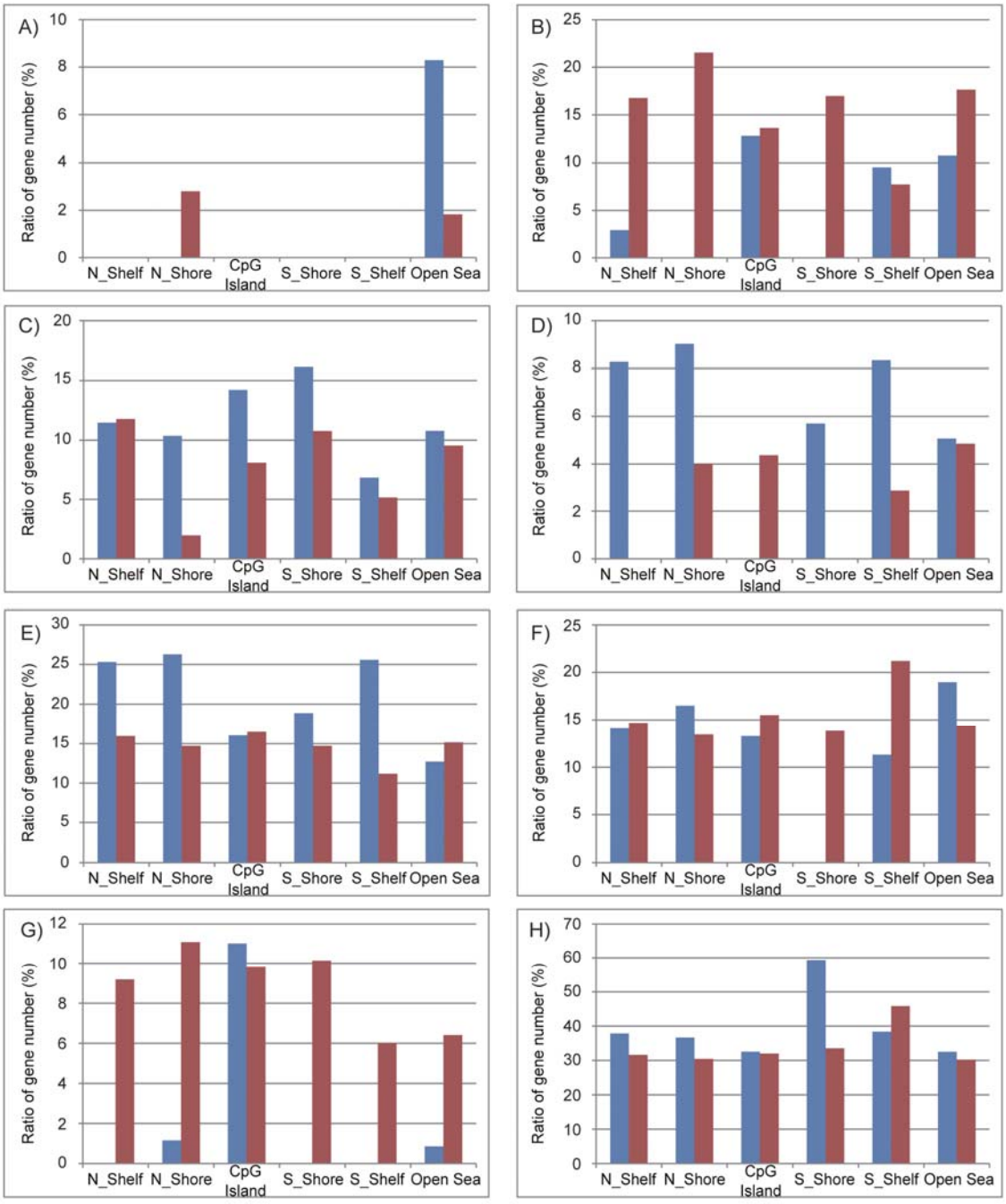

Fig. 6. The characterization of genes hosting differentially methylated CpG sites in the CpG site subcategories.

The same type of GO analyses shown in Fig. 5 was applied to six CpG subcategories (N_Shelf, N_Shore, CpG island, S_Shore, S_Shelf, and the open sea). S3 Table shows

the number of genes analyzed and classified.

Hypomethylation observed in the open sea was frequently associated with the up-regulation of genes related to immune response

Next, we performed an integrated analysis of HumanMethylation450 BeadChip and gene expression profiles to investigate potential functional effects of DNA methylation on gene expression in replicative senescence. Most methylation changes were unlikely to have a significant impact on gene expression (S2 Fig). Out of 212,885 probes located within 8 kb distance from a TSS of RefSeq genes, 1,596 CpG sites were differentially methylated along with the altered expression of the nearest genes to these CpG sites: 1,101 hyper- and 495 hypo-methylated CpG sites for which the nearest genes were down- and up-regulated, respectively, upon senescence (S4 Table). The genes nearest to these 1,596 differentially methylated CpG sites were subjected to GO analysis using DAVID. Those genes with up-regulated expression that were in a hypomethylated state in close proximity (within 8 kb) to their TSS were involved in “immune response” and “cell death” as ranked in the top 10

terms (Table 2). The immune response-related genes included *MHC II*, and the cell death-related genes included *FAS* and *oxidized low density lipoprotein receptor 1 (OLR1)*. In contrast, those genes with down-regulated expression that were in a hypermethylated state in close proximity to their TSS were categorized into several categories such as “development” and “cell cycle”.

We also assessed the distribution of the distances between each of the 1,596 differentially methylated CpG sites and the nearest TSS. In this analysis, we classified genes into two subcategories based on promoter types, CGI and non-CGI promoters. The number of probes for all CpG sites within CGI and non-CGI promoters on the array were 204,829 and 94,432 respectively (Fig. 7A). The number of probes located within 1 kb distance to the TSS was 186,998 (62%). The 1,101 hypermethylated CpG sites for which the nearest gene was down-regulated upon replicative senescence consisted of 744 and 357 CpG sites within CGI and non-CGI promoters, respectively. The hypermethylated CpG sites tended to be located more frequently in CGI promoters than in non-CGI promoters, and located close to the TSS: 630 out of 1,101 (57%) within 1 kb distance (Fig. 7B). The distribution patterns were

similar between all CpG sites (Fig. 7A) and 1,101 hypermethylated CpG sites (Fig. 7B). In sharp contrast, 495 hypomethylated CpG sites for which the nearest gene was up-regulated were mainly located in non-CGI promoters (Fig. 7C). Within 1 kb distance of the TSS, 202 hypomethylated CpG sites, for which the nearest gene was up-regulated upon replicative senescence, consisted of 36 and 166 CpG sites within CGI and non-CGI promoters, respectively (Fig. 7C). This distribution pattern was similar to that of a subset of hypomethylated CpG sites, for which the nearest gene was up-regulated and related to "immune response" (Fig. 7D). This result suggests the possibility that DNA methylation on the promoter modulates the expression of a subset of "immune response" genes in replicative senescence.

Table 2. GO analysis of genes showing the relationship between methylation and gene expression level in replicative senescence.

Rank	Hypomethylation & up-regulated gene expression (n=351)		Hypermethylation & down-regulated gene expression (n=516)	
	GO term categories	Enrichment Score	GO term categories	Enrichment Score
1	Response to stimulus	3.20	Developmental process	7.08
2	Immune response	3.19	Organ development	5.14
3	Inflammatory response	2.73	Lung alveolus development	3.69
4	Response to hormone stimulus, Response to corticosteroid stimulus	2.50	Embryonic development	3.64
5	Response to nutrient levels, Response to extracellular stimulus	2.30	Cell cycle	3.16
6	Regulation of transport	1.69	Negative regulation of transcription	3.11
7	Developmental process	1.62	Epithelial tube morphogenesis	2.70
8	Cell death	1.37	Mesenchymal cell development	2.47
9	Actin cytoskeleton organization	1.26	Ear development	2.46
10	Negative/positive regulation of kinase activity	1.25	Positive regulation of transcription, DNA-dependent, positive regulation of metabolic	2.34

*More than 1.3 of enrichment scores gave less than 0.05 p-values.

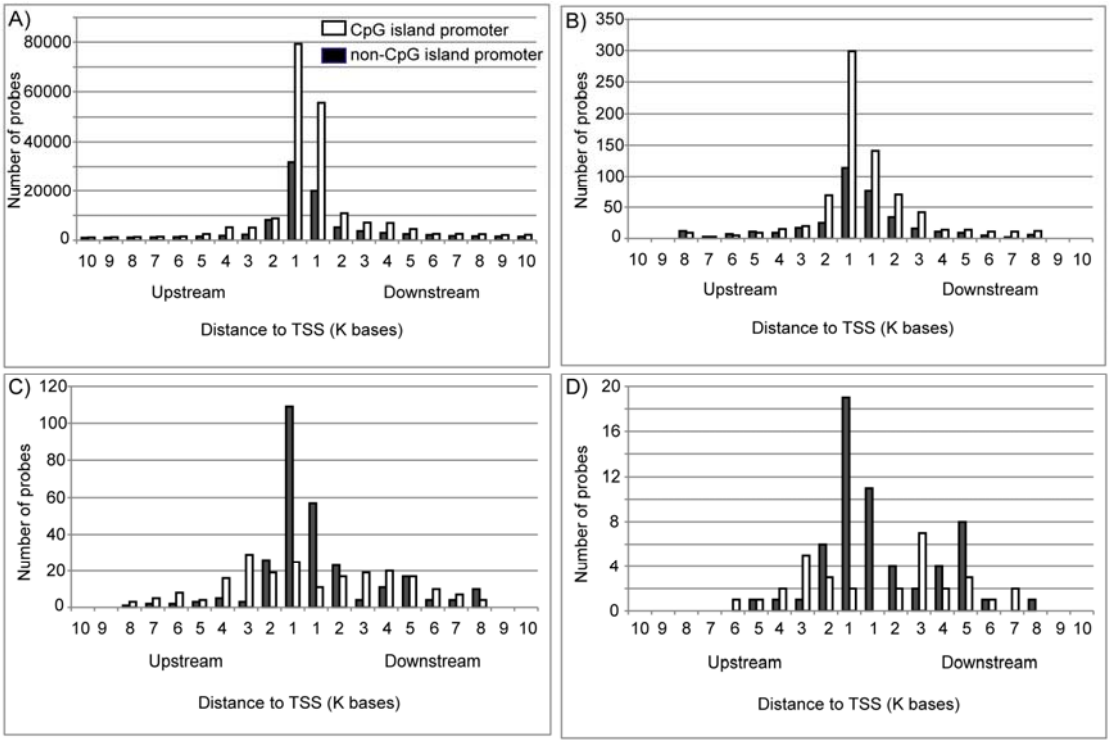

Fig. 7. Distribution patterns of the distances between CpG sites and the nearest TSS.

Distribution patterns for all 299,261 CpG probes on the HumanMethylation450 BeadChip (A), 1,101 hypermethylated CpG sites for which the nearest gene was down-regulated upon replicative senescence (B), 495 hypomethylated CpG sites for which the nearest gene was up-regulated upon replicative senescence (C), and 90 hypomethylated CpG sites for which the nearest gene was up-regulated upon replicative senescence and related to immune response (D) are shown.

DNA methylation affected the expression of miRNAs and the target genes during replicative senescence

A HumanMethylation450 BeadChip includes 3,436 probes related to miRNA. In replicatively senescent TIG-3 cells, 98 CpG sites corresponding to 66 miRNAs were hypomethylated, whereas 102 CpG sites corresponding to 62 miRNAs were hypermethylated (S5 Table). The expression levels of miRNAs were examined using Human miRNA microarray (Release 21.0), where 2,549 human miRNAs were represented. During replicative senescence, 178 miRNAs (fold-change >= ±1.5) showed up- or down-regulated (data not shown). To select miRNAs for which expression seemed to be regulated by DNA methylation, we compared the methylation changes of CpG sites related to miRNA with the miRNA expression changes. Among 18 miRNAs selected, seven miRNAs showed a decrease in expression accompanied with a hypermethylated CpG site in the promoters (S6 Table). This result was consistent with a previous report using IMR 90 cells, where the expression levels of six of the seven miRNAs were down-regulated during replicative senescence [40]. In contrast, no miRNAs showed an increase in expression along with a hypomethylated CpG site in the promoters. We next searched

for candidate genes targeted by the seven miRNAs using TargetScan Human Release 7.0, and these genes were further selected by more than two miRNAs and the targeted gene expression levels based on our microarray data. As a result, we identified 27 genes for which expression seemed to be indirectly regulated by DNA methylation on the promoters of targeting miRNAs (Table 3). The genes encoding IL-6 signal transducer (*IL6ST*) and Zinc finger matrin-type 3 (*ZMAT3*) were included in the targeted genes.

Table 3. Targeted genes mediated in part by miRNAs, with miRNA expression regulated via methylation in the promoter regions.

Targeted gene symbol	Gene expression (fold-change)	miRNAs of regulating targeted gene		
EIF4EBP2	3.0	hsa-miR-7-5p	hsa-miR-193a-5p	hsa-miR-335-5p
HECW2	4.2	hsa-miR-7-5p	hsa-miR-25-3p	hsa-miR-505-3p
CADM1	8.2	hsa-miR-7-5p	hsa-miR-505-3p	
CNNM2	2.9	hsa-miR-335-5p	hsa-miR-505-3p	
CPEB2	2.6	hsa-miR-7-5p	hsa-miR-505-3p	
CRY2	2.2	hsa-miR-7-5p	hsa-miR-17-5p	
DAAM1	2.5	hsa-miR-130b-3p	hsa-miR-335-5p	
DGKH	2.5	hsa-miR-130b-3p	hsa-miR-505-3p	
DOK6	2.2	hsa-miR-17-5p	hsa-miR-335-5p	
EGR2	2.8	hsa-miR-17-5p	hsa-miR-25-3p	
FAM134C	2.2	hsa-miR-17-5p	hsa-miR-335-5p	
GRIN2A	2.0	hsa-miR-7-5p	hsa-miR-130b-3p	
HPCAL4	7.6	hsa-miR-7-5p	hsa-miR-335-5p	
IL6ST	2.2	hsa-miR-130b-3p	hsa-miR-505-3p	
KLHL28	2.4	hsa-miR-7-5p	hsa-miR-335-5p	
MEF2D	2.7	hsa-miR-335-5p	hsa-miR-505-3p	
MYO1D	5.9	hsa-miR-193a-5p	hsa-miR-335-5p	
NR4A3	2.1	hsa-miR-7-5p	hsa-miR-335-5p	
OXR1	2.9	hsa-miR-7-5p	hsa-miR-17-5p	
PGM2L1	4.8	hsa-miR-17-5p	hsa-miR-130b-3p	
PIP4K2C	2.1	hsa-miR-25-3p	hsa-miR-505-3p	
PPARGC1B	2.6	hsa-miR-7-5p	hsa-miR-505-3p	
RAB11FIP5	2.8	hsa-miR-7-5p	hsa-miR-17-5p	
RNF141	2.4	hsa-miR-7-5p	hsa-miR-335-5p	
SEMA6D	5.9	hsa-miR-7-5p	hsa-miR-193a-5p	
ZDHHC8	5.2	hsa-miR-17-5p	hsa-miR-335-5p	
ZMAT3	3.4	hsa-miR-7-5p	hsa-miR-130b-3p	

Discussion

In this study, Infinium HumanMethylation27 BeadChips (Illumina) were used to determine the DNA methylation levels in three types of senescent cells. We found that only replicatively senescent cells were differentially methylated, whereas prematurely senescent ones (RIS and SVts8) were not (Fig. 3 and Table 1). These results were in good agreement with previous studies showing DNA methylation changes in aged tissues and cells [23, 32, 35, 56]. There are several reasons why the DNA methylation profile is strongly modified during replicative senescence and not during premature senescence. Firstly, errors may accumulate due to repeated cell division. Laird *et al.* evaluated the fidelity of transmission of the DNA methylation state in the CpG island of the *FMR1* gene in normal human lymphocytes using hairpin-bisulfite PCR [57]. Although relatively high fidelity of inheritance of the methylated state of cytosine was found, the results clearly showed that errors in maintaining DNA methylation occurred to some extent in every DNA replication. When culturing TIG-3 cells from PDL 36 to PDL 85, the cells would proliferate by approximately 2^50 times. In contrast, as RIS and senescent SVts8 cells were rapidly induced to a senescent state,

prematurely senescent cells would not have enough rounds of cell division to accumulate any errors. Secondly, reduced activity of DNA methyltransferase 1 (DNMT1), which primarily maintains DNA methylation patterns during replication, may increase the incidence of errors. The expression profiles in this study exhibited a marked decrease in *DNMT1* in replicatively senescent cells (0.23-fold reduction, data not shown), whereas the expression levels of *DNMT1* in RIS (0.70-fold reduction, data not shown) and senescent SVts8 (0.80-fold reduction, data not shown) were slightly reduced. This is consistent with the results reported by Kaneda *et al.*, who reported that DNA methylation was not altered in RIS using methylated DNA immunoprecipitation (MeDIP) sequencing and bisulfite sequencing, and the *Dnmt1* expression level was not altered in RIS, or during 3 passages (passage 2 to 5) using mouse embryonic fibroblasts [23]. Thirdly, a marked decrease in Ten-eleven translocation 1 (TET1) expression could alter DNA methylation patterns. Recent studies have suggested active DNA demethylation is mediated by TET, the enzyme that converts 5-methylcytosine (5mC) to 5-hydroxymethylcytosine (5hmC), 5-formylcytosine (5fc), and 5-carboxylcytosine (5caC) [58-61]. There are three

TET proteins: TET1, TET2 and TET3. The expression levels of *TET1* and *TET3* genes, but not *TET2*, reportedly decrease along with aging, and *TET3* expression is important for decreasing genomic 5hmC during aging in human T cells [62]. In replicatively senescent TIG-3 cells, the expression levels of the *TET1* gene were drastically decreased, although we have no expression data for the TET3 gene due to a lack of TET3 probes in the expression array. A recent study showed that *Tet1*/*Tet2* double-knockout mouse embryonic fibroblasts (MEFs) had defects in maintaining hypomethylation and resulted in hypermethylation of DNA methylation canyons where developmental genes are associated [63]. Taken together, methylation changes during senescence would require many rounds of cell division and the decreased activities of DNA methyltransferase and methylcytosine deoxygenase, such as DNMT1 and TET1, might produce the altered methylation patterns within long-term culture.

Since most CpG islands at TSS are generally not methylated, the hypermethylation at CpG islands, especially near TSS, has been investigated extensively. Thus, it was revealed that hypermethylation of CpG islands in the region around TSS and the first exon plays a role in gene

silencing [58, 64]. Several papers showed hypermethylation at CpG islands in replicative senescence, corroborating our results [65, 66]. In addition, a recent study revealed that hypermethylation at shore inhibits gene expression of tumor suppressors in breast cancer [67]. Since our data agree with those reports, hypermethylation at CpG islands and shore would contribute to down-regulation of gene expression in replicative senescence. On the other hand, because there is a tendency that hypomethylation in senescence is caused by general dysfunction of methylation [34], the role of hypomethylation in senescence remains unexplored [58, 64]. However, recent studies revealed that hypomethylation occurs not only passively but also actively, and that active DNA demethylation triggers transcription [60, 61, 68]. We found that hypomethylation observed in the open sea was frequently associated with the up-regulation of genes related to immune response. When the genes hosting hypomethylated CpG sites were classified into six CpG subcategories using annotated GO terms, genes related to "immune response" were enriched only in the genes hosting hypomethylated CpG sites in the "open sea" (Fig. 6A). Consistent with the results, the promoter types of genes categorized as "immune response" were mainly non-CGI promoters

(Fig. 7D), although, the probes in the HumanMethylation450 BeadChip covered much more CpG island promoter genes than non-CpG island promoter genes (Fig. 7A). In contrast, genes categorized into other groups, namely “metabolic process”, “transport”, “cell adhesion”, “development”, “signal transduction”, and “transcription”, exhibited hypermethylation rather than hypomethylation in the CpG sites close to the TSS (S3 Table).

To corroborate the role of methylation in the regulation of gene expression during replicative senescence, integrated analysis of methylation and gene expression was performed. Although only 0.7% (1,596 in 212,885) of the probes showed a relationship between DNA methylation and gene expression, the top ten GO terms of integrated results agreed with the GO terms of gene expression in replicative senescence. Therefore, it is likely that the expression of some genes contributing to establishment of a senescent state such as cell cycle arrest and active immune response is partially regulated by DNA methylation.

Among the GO terms associated with hypomethylation as to site-subcategories, hypomethylation of the genes related to “immune response” was almost always detected at open sea (Fig. 6A). Furthermore,

although the probes in an Infinium HumanMethylation450 BeadChip cover much more CpG island promoter than non-CpG island promoter genes (Fig. 7A), the genes categorized as “immune response” ones mainly include non-CpG island promoters (Fig. 7D). These results suggested that hypomethylation at open sea in replicatively senescent cells contributes to the regulation of genes with non-CpG island promoters, especially those associated with the immune response. Cellular senescence was reported to be related with the immune response, which is known as SASP [15]. In addition, several papers indicated the association between DNA methylation and inflammatory genes [69-71]. N.F.P. Oliveira, *et al.* [69] reported that DNA hypomethylation at *IL8* gene promoters (non-CpG island promoters) is related to inflammation in the oral mucosae of smokers with periodontitis. These facts suggest that hypomethylation at open sea may contribute to increases in immune response gene expression associated with a senescent state.

Our study on the relationship of gene expression and methylation change during senescence implied an association between aged-related diseases and the genes regulated by DNA hypomethylation. For example,

MHC II, which has non-CpG island promoters exhibiting hypomethylation and whose expression is up-regulated during replicative senescence, presents exogenous and endogenous antigens [72] to CD4+ T cells. CD4+ T cells differentiate into Th1, Th2 and Th17 cells for humoral immunity [73]. The expression of IL-6, which is one of the SASP factors [14, 15, 74], and that of transforming growth factor beta (TGF-β) were found to be up-regulated (IL-6, 11.5-fold change; TGFB2, 17.0-fold change) in our data, and both are necessary for Th17 cell development [75]. Moreover, Th17 was reported to be associated with autoimmune disease [75, 76]. In replicative senescence, up-regulated *MHC II* with hypomethylation under high IL-6 and TGF-β may be one of the key factors for development of Th17 associating with autoimmune disease.

Currently we cannot explain the mechanism by which hypomethylation in the non-CpG promoter occurs in a certain portion of the "immune response"-related genes during replicative senescence. We speculate that TET2 may play a role in this regulation. As mentioned above, TET proteins contribute to active DNA demethylation. In our data, the expression levels of one of the *TET2* probes showed a 2-fold increase in

replicatively senescent cells and senescent SVts8 cells, whereas no increase in *TET2* expression was detected in the RIS cells. Unlike TET1 and TET3, TET2 does not have a CXXC domain, which is required for binding to the CpG site [77, 78]. These results suggest that collaboration between TET2 and its associated factor(s) may be required for DNA binding and demethylation. In fact, TET2 was reported to need a cofactor for binding to DNA [61]. During differentiation of helper T (Th) cells, TET2 induced DNA demethylation at the loci of key cytokine genes in a lineage-specific transcription factor-dependent manner and promoted signature cytokine expression in Th1 and Th17 cells [79]. Our *IL17A* gene data also showed hypomethylation at open sea and a slight gene expression increase (1.9-fold change in replicative senescence, but 1.4-fold change in RIS and 1.5-fold change in senescent SVts8), and association between the immune response and senescence as described above. Depending on the cofactor, TET2 may bind to non-CGI promoters in senescence-associated genes, and increase gene expression. Further studies are needed to investigate the effects of TET2 on hypomethylation at the specific CpG sites and its interacting factor(s) during senescence.

Recently, senescence-associated miRNAs (SA-miRNAs) have been reported to regulate genes associated with senescence [40-44]. We examined the effects of DNA methylation in the promoter regions of miRNAs on miRNA expression using human miRNA expression microarray and further selected miRNAs that likely affected the predicted gene expression. As a result, we identified seven miRNAs and 27 targeted genes (Table 3). These genes included eukaryotic translation initiation factor 4E binding protein 2 (*EIF4EBP2*), which inhibits translation initiation [80], and cryptochrome circadian clock 2 (*CRY2*), which is a key component in regulating circadian rhythm [81]. Among the 27 genes, the IL-6 signal transducer (*IL6ST*) and zinc finger matrin-type 3 (*ZMAT3*) are involved in immune response. *IL6ST*, which is supposed to be up-regulated by decreased levels of has-miR-130b-3p and has-miR-505-3p, encodes glycoprotein 130 (gp130) [82]. The protein gp130 is a signal transducer shared by many cytokines including IL-6, one of the SASP factors [74], IL-11, IL-27, and oncostatin-M [83-85]. In addition, *ZMAT3*, a predicted gene regulated by has-miR-7-5p and has-miR-130b-3p, encodes a double-stranded-RNA-binding zinc finger protein Wig-1 (for wild-type p53-induced gene 1). Wig-1, a transcriptional

target of p53, stabilizes p53 by binding to the 3' UTR of p53 mRNA and protecting it from deadenylation [86]. A high level of p53 triggers cell cycle arrest, senescence and apoptosis, and efficiently inhibits tumor development [11, 13, 87]. In addition to the p53 transcription factor, miRNAs with expression regulated by DNA methylation via their promoter regions may also contribute to *ZMAT3* expression. MiR-34 is one of the SA-miRNAs and is up-regulated by p53 [40, 41, 45, 46, 88, 89]. Although increased levels of miRNA-34 were detected upon replicative senescence, the methylation changes (Δβ cut-off was ±0.2) in the promoter regions of miRNA-34 were not included in our data (data not shown).

In this study, we investigated the possibility of regulation by DNA methylation during senescence. We found that hypomethylation in the open sea may contribute to the up-regulation of genes related to immune response. Several miRNAs targeting genes associated with a senescent state seem to regulate expression by DNA methylation in the promoter regions. However, we have to consider the possibility that DNA methylation results from alteration of gene expression. To investigate this possibility, we need to collect more data and explore the mechanism of methylation and

demethylation change. Moreover, in order to reveal the whole mechanism of DNA methylation, we also need to focus on the methylation profile in hypomethylation and outside of the TSS and CpG islands.

Conclusion

Three types of senescent TIG-3 cells showed similar biological outcomes, but the regulatory mechanisms were different. Replicatively senescent cells showed sequential DNA methylation changes, but prematurely senescent RIS and SVts8 cells did not. In replicative senescence, hypomethylation with up-regulated gene expression often occurred in the open sea. Moreover, hypomethylation was observed in non-CGI promoters of genes related to the immune response. These results suggested that hypomethylation in the open sea regulates the expression of a certain portion of immune-related genes in replicative senescence. In addition, several miRNAs that seemed to have expression levels regulated in part by DNA methylation may also contribute to the expression of senescence-associated genes.

List of Abbreviations

COBRA	combined bisulfite restriction analysis
CGI	CpG island
CRY2	cryptochrome circadian clock 2
DAVID	Database for Annotation, Visualization and Integrated Discovery
DDR	DNA damage response
DNMT1	DNA methyltransferase 1
EIF4EBP2	eukaryotic translation initiation factor 4E binding protein 2
FBS	fetal bovine serum
GO	Gene ontology
gp130	glycoprotein 130
H3K9me3	trimethylated histone H3 at lysine9
H3K27me3	trimethylated histone H3 at lysine 27
H3K4me3	trimethylation of histone H3 at lysine 4
IL	interleukin
IL6ST	IL-6 signal transducer
MeDIP	mouse embryonic fibroblasts
MEFs	methylated DNA immunoprecipitation

miRNA	micro RNA
OLR1	oxidized low density lipoprotein receptor 1
PDL	population doubling level
RB	retinoblastoma
RIS	*ras*-induced senescent
ROS	reactive oxygen species
SA-ß-Gal	senescence-associated beta-galactosidase
SAHF	senescence-associated heterochromatic foci
SA-miRNAs	senescence-associated miRNAs
SASP	senescence-associated secretory phenotype
SV	simian virus
TET	Ten-eleven translocation
TSS	transcription start site
UTR	untranslated region
ZMAT3	Zinc finger matrin-type 3
5caC	5-carboxylcytosine
5fc	5-formylcytosine
5hmC	5-hydroxymethylcytosine

5mC	5-methylcytosine

Acknowledgments

I heartily appreciate the knowledge and guidance provided by Dr. Kayoko Maehara, who has kindly assisted my completion of this project. This doctoral thesis would not have been possible without her help. I would also like to thank Dr. Yoshiro Kobayashi for giving a lot of advice and proofreading my English. Furthermore, I'm grateful to Dr. Kazuhiko Nakabayashi, Dr. Kohji Okamura and Dr. Arisa Igarashi for helping the data analysis and writing my manuscript.

Finally, I would like to show my gratitude to my family and friends. Their understanding and support were very helpful and encouraging.

References

1. Hayflick L, Moorhead PS. The serial cultivation of human diploid cell strains. Exp Cell Res. 1961;25:585-621. PubMed PMID: 13905658.
2. Hayflick L. The limited in vitro lifetime of human diploid cell strains. Exp Cell Res. 1965;37:614-636. PubMed PMID: 14315085.
3. Kuilman T, Michaloglou C, Mooi WJ, Peeper DS. The essence of senescence. Genes Dev. 2010;24(22):2463-2479. doi: 10.1101/gad.1971610. PubMed PMID: 21078816.
4. Harley CB, Futcher AB, Greider CW. Telomeres shorten during ageing of human fibroblasts. Nature. 1990;345(6274):458-460. doi: 10.1038/345458a0. PubMed PMID: 2342578.
5. d'Adda di Fagagna F, Reaper PM, Clay-Farrace L, Fiegler H, Carr P, Von Zglinicki T, et al. A DNA damage checkpoint response in telomere-initiated senescence. Nature. 2003;426(6963):194-198. doi: 10.1038/nature02118. PubMed PMID: 14608368.
6. Serrano M, Lin AW, McCurrach ME, Beach D, Lowe SW. Oncogenic ras provokes premature cell senescence associated with accumulation of p53 and p16INK4a. Cell. 1997;88(5):593-602. PubMed PMID: 9054499.
7. Takahashi A, Ohtani N, Yamakoshi K, Iida S, Tahara H, Nakayama K, et al. Mitogenic signalling and the p16INK4a-Rb pathway cooperate to enforce irreversible cellular senescence. Nat Cell Biol. 2006;8(11):1291-1297. doi: 10.1038/ncb1491. PubMed PMID: 17028578.
8. Tsuyama N, Miura M, Kitahira M, Ishibashi S, Ide T. SV40 T-antigen is required for maintenance of immortal growth in SV40-transformed human fibroblasts. Cell Struct Funct. 1991;16(1):55-62. PubMed PMID: 1851674.
9. Ben-Porath I, Weinberg RA. The signals and pathways activating cellular senescence. Int J Biochem Cell Biol. 2005;37(5):961-976. doi: 10.1016/j.biocel.2004.10.013. PubMed PMID: 15743671.
10. Salama R, Sadaie M, Hoare M, Narita M. Cellular senescence and its effector programs. Genes Dev. 2014;28(2):99-114. doi: 10.1101/gad.235184.113. PubMed PMID: 24449267.
11. Beausejour CM, Krtolica A, Galimi F, Narita M, Lowe SW, Yaswen P, et al. Reversal of human cellular senescence: roles of the p53 and p16 pathways. EMBO J. 2003;22(16):4212-4222. doi: 10.1093/emboj/cdg417. PubMed PMID: 12912919.
12. Collado M, Blasco MA, Serrano M. Cellular senescence in cancer and aging. Cell. 2007;130(2):223-233. doi: 10.1016/j.cell.2007.07.003. PubMed PMID: 17662938.
13. Campisi J. Cellular senescence as a tumor-suppressor mechanism. Trends Cell Biol. 2001;11(11):S27-31. PubMed PMID: 11684439.

14. Campisi J. Aging, cellular senescence, and cancer. Annu Rev Physiol. 2013;75:685-705. doi: 10.1146/annurev-physiol-030212-183653. PubMed PMID: 23140366.
15. Coppe JP, Patil CK, Rodier F, Sun Y, Munoz DP, Goldstein J, et al. Senescence-associated secretory phenotypes reveal cell-nonautonomous functions of oncogenic RAS and the p53 tumor suppressor. PLoS Biol. 2008;6(12):2853-2868. doi: 10.1371/journal.pbio.0060301. PubMed PMID: 19053174.
16. Wu Z, Nakanishi H. Lessons from Microglia Aging for the Link between Inflammatory Bone Disorders and Alzheimer's Disease. J Immunol Res. 2015;2015:1-9. doi: 10.1155/2015/471342. PubMed PMID: 26078980.
17. Strahl BD, Allis CD. The language of covalent histone modifications. Nature. 2000;403(6765):41-45. doi: 10.1038/47412. PubMed PMID: 10638745.
18. Narita M, Nunez S, Heard E, Narita M, Lin AW, Hearn SA, et al. Rb-mediated heterochromatin formation and silencing of E2F target genes during cellular senescence. Cell. 2003;113(6):703-716. PubMed PMID: 12809602.
19. Narita M, Narita M, Krizhanovsky V, Nunez S, Chicas A, Hearn SA, et al. A novel role for high-mobility group a proteins in cellular senescence and heterochromatin formation. Cell. 2006;126(3):503-514. doi: 10.1016/j.cell.2006.05.052. PubMed PMID: 16901784.
20. Zhang W, Hu D, Ji W, Yang L, Yang J, Yuan J, et al. Histone modifications contribute to cellular replicative and hydrogen peroxide-induced premature senescence in human embryonic lung fibroblasts. Free Radic Res. 2014;48(5):550-559. doi: 10.3109/10715762.2014.893580. PubMed PMID: 24528089.
21. Shah PP, Donahue G, Otte GL, Capell BC, Nelson DM, Cao K, et al. Lamin B1 depletion in senescent cells triggers large-scale changes in gene expression and the chromatin landscape. Genes Dev. 2013;27(16):1787-1799. doi: 10.1101/gad.223834.113. PubMed PMID: 23934658.
22. Bracken AP, Kleine-Kohlbrecher D, Dietrich N, Pasini D, Gargiulo G, Beekman C, et al. The Polycomb group proteins bind throughout the INK4A-ARF locus and are disassociated in senescent cells. Genes Dev. 2007;21(5):525-530. doi: 10.1101/gad.415507. PubMed PMID: 17344414.
23. Kaneda A, Fujita T, Anai M, Yamamoto S, Nagae G, Morikawa M, et al. Activation of Bmp2-Smad1 signal and its regulation by coordinated alteration of H3K27 trimethylation in Ras-induced senescence. PLoS Genet. 2011;7(11):e1002359. doi: 10.1371/journal.pgen.1002359. PubMed PMID: 22072987.
24. Takahashi A, Imai Y, Yamakoshi K, Kuninaka S, Ohtani N, Yoshimoto S, et al. DNA damage signaling triggers degradation of histone methyltransferases through APC/C(Cdh1) in senescent cells. Mol Cell. 2012;45(1):123-131. doi:

10.1016/j.molcel.2011.10.018. PubMed PMID: 22178396.

25. Razin A, Riggs AD. DNA methylation and gene function. Science. 1980;210(4470):604-610. PubMed PMID: 6254144.
26. Xu W, Wang F, Yu Z, Xin F. Epigenetics and Cellular Metabolism. Genet Epigenet. 2016;8:43-51. doi: 10.4137/geg.s32160. PubMed PMID: 27695375.
27. Fatemi M, Pao MM, Jeong S, Gal-Yam EN, Egger G, Weisenberger DJ, et al. Footprinting of mammalian promoters: use of a CpG DNA methyltransferase revealing nucleosome positions at a single molecule level. Nucleic Acids Res. 2005;33(20):e176. doi: 10.1093/nar/gni180. PubMed PMID: 16314307.
28. Goldberg AD, Allis CD, Bernstein E. Epigenetics: a landscape takes shape. Cell. 2007;128(4):635-638. doi: 10.1016/j.cell.2007.02.006. PubMed PMID: 17320500.
29. Zhang Y, Elgizouli M, Schottker B, Holleczek B, Nieters A, Brenner H. Smoking-associated DNA methylation markers predict lung cancer incidence. Clin Epigenetics. 2016;8(127):1-12. doi: 10.1186/s13148-016-0292-4. PubMed PMID: 27924164.
30. Asada K, Kotake Y, Asada R, Saunders D, Broyles RH, Towner RA, et al. LINE-1 hypomethylation in a choline-deficiency-induced liver cancer in rats: dependence on feeding period. J Biomed Biotechnol. 2006;2006(1):1-6. doi: 10.1155/jbb/2006/17142. PubMed PMID: 16877811.
31. Varley KE, Gertz J, Bowling KM, Parker SL, Reddy TE, Pauli-Behn F, et al. Dynamic DNA methylation across diverse human cell lines and tissues. Genome Res. 2013;23(3):555-567. doi: 10.1101/gr.147942.112. PubMed PMID: 23325432.
32. Horvath S, Zhang Y, Langfelder P, Kahn RS, Boks MP, van Eijk K, et al. Aging effects on DNA methylation modules in human brain and blood tissue. Genome Biol. 2012;13(10):1-18. doi: 10.1186/gb-2012-13-10-r97. PubMed PMID: 23034122.
33. Koch CM, Wagner W. Epigenetic biomarker to determine replicative senescence of cultured cells. Methods Mol Biol. 2013;1048:309-321. doi: 10.1007/978-1-62703-556-9_20. PubMed PMID: 23929112.
34. Koch CM, Suschek CV, Lin Q, Bork S, Goergens M, Joussen S, et al. Specific age-associated DNA methylation changes in human dermal fibroblasts. PLoS One. 2011;6(2):e16679. doi: 10.1371/journal.pone.0016679. PubMed PMID: 21347436.
35. Christensen BC, Houseman EA, Marsit CJ, Zheng S, Wrensch MR, Wiemels JL, et al. Aging and environmental exposures alter tissue-specific DNA methylation dependent upon CpG island context. PLoS Genet. 2009;5(8):e1000602. doi: 10.1371/journal.pgen.1000602. PubMed PMID: 19680444.
36. Fraga MF, Ballestar E, Paz MF, Ropero S, Setien F, Ballestar ML, et al. Epigenetic

differences arise during the lifetime of monozygotic twins. Proc Natl Acad Sci U S A. 2005;102(30):10604-10609. doi: 10.1073/pnas.0500398102. PubMed PMID: 16009939.

37. Jjingo D, Conley AB, Yi SV, Lunyak VV, Jordan IK. On the presence and role of human gene-body DNA methylation. Oncotarget. 2012;3(4):462-474. PubMed PMID: 22577155.
38. Cheng AM, Byrom MW, Shelton J, Ford LP. Antisense inhibition of human miRNAs and indications for an involvement of miRNA in cell growth and apoptosis. Nucleic Acids Res. 2005;33(4):1290-1297. doi: 10.1093/nar/gki200. PubMed PMID: 15741182.
39. Slaby O, Svoboda M, Michalek J, Vyzula R. MicroRNAs in colorectal cancer: translation of molecular biology into clinical application. Mol Cancer. 2009;8:102. doi: 10.1186/1476-4598-8-102. PubMed PMID: 19912656.
40. Dhahbi JM, Atamna H, Boffelli D, Magis W, Spindler SR, Martin DI. Deep sequencing reveals novel microRNAs and regulation of microRNA expression during cell senescence. PLoS One. 2011;6(5):e20509. doi: 10.1371/journal.pone.0020509. PubMed PMID: 21637828.
41. Lafferty-Whyte K, Cairney CJ, Jamieson NB, Oien KA, Keith WN. Pathway analysis of senescence-associated miRNA targets reveals common processes to different senescence induction mechanisms. Biochim Biophys Acta. 2009;1792(4):341-352. doi: 10.1016/j.bbadis.2009.02.003. PubMed PMID: 19419692.
42. Taguchi YH. Inference of Target Gene Regulation via miRNAs during Cell Senescence by Using the MiRaGE Server. Aging Dis. 2012;3(4):301-306. PubMed PMID: 23185711.
43. Overhoff MG, Garbe JC, Koh J, Stampfer MR, Beach DH, Bishop CL. Cellular senescence mediated by p16INK4A-coupled miRNA pathways. Nucleic Acids Res. 2014;42(3):1606-1618. doi: 10.1093/nar/gkt1096. PubMed PMID: 24217920.
44. Li CW, Wang WH, Chen BS. Investigating the specific core genetic-and-epigenetic networks of cellular mechanisms involved in human aging in peripheral blood mononuclear cells. Oncotarget. 2016;7(8):8556-8579. doi: 10.18632/oncotarget.7388. PubMed PMID: 26895224.
45. Tazawa H, Tsuchiya N, Izumiya M, Nakagama H. Tumor-suppressive miR-34a induces senescence-like growth arrest through modulation of the E2F pathway in human colon cancer cells. Proc Natl Acad Sci U S A. 2007;104(39):15472-15477. doi: 10.1073/pnas.0707351104. PubMed PMID: 17875987.
46. He X, He L, Hannon GJ. The guardian's little helper: microRNAs in the p53 tumor suppressor network. Cancer Res. 2007;67(23):11099-11101. doi: 10.1158/0008-5472.can-07-2672. PubMed PMID: 18056431.
47. Christoffersen NR, Shalgi R, Frankel LB, Leucci E, Lees M, Klausen M, et al. p53-independent upregulation of miR-34a during oncogene-induced senescence

represses MYC. Cell Death Differ. 2010;17(2):236-245. doi: 10.1038/cdd.2009.109. PubMed PMID: 19696787.

48. Ayala-Ortega E, Arzate-Mejia R, Perez-Molina R, Gonzalez-Buendia E, Meier K, Guerrero G, et al. Epigenetic silencing of miR-181c by DNA methylation in glioblastoma cell lines. BMC Cancer. 2016;16(226):1-12. doi: 10.1186/s12885-016-2273-6. PubMed PMID: 26983574.
49. Asuthkar S, Velpula KK, Chetty C, Gorantla B, Rao JS. Epigenetic regulation of miRNA-211 by MMP-9 governs glioma cell apoptosis, chemosensitivity and radiosensitivity. Oncotarget. 2012;3(11):1439-1454. doi: 10.18632/oncotarget.683. PubMed PMID: 23183822.
50. Yin H, Song P, Su R, Yang G, Dong L, Luo M, et al. DNA Methylation mediated down-regulating of MicroRNA-33b and its role in gastric cancer. Sci Rep. 2016;6(18824):1-12. doi: 10.1038/srep18824. PubMed PMID: 26729612.
51. Maehara K, Takahashi K, Saitoh S. CENP-A reduction induces a p53-dependent cellular senescence response to protect cells from executing defective mitoses. Mol Cell Biol. 2010;30(9):2090-2104. doi: 10.1128/mcb.01318-09. PubMed PMID: 20160010.
52. Chen C, Okayama H. High-efficiency transformation of mammalian cells by plasmid DNA. Mol Cell Biol. 1987;7(8):2745-2752. PubMed PMID: 3670292.
53. Bibikova M, Le J, Barnes B, Saedinia-Melnyk S, Zhou L, Shen R, et al. Genome-wide DNA methylation profiling using Infinium(R) assay. Epigenomics. 2009;1(1):177-200. doi: 10.2217/epi.09.14. PubMed PMID: 22122642.
54. Bibikova M, Barnes B, Tsan C, Ho V, Klotzle B, Le JM, et al. High density DNA methylation array with single CpG site resolution. Genomics. 2011;98(4):288-295. doi: 10.1016/j.ygeno.2011.07.007. PubMed PMID: 21839163.
55. Price ME, Cotton AM, Lam LL, Farre P, Emberly E, Brown CJ, et al. Additional annotation enhances potential for biologically-relevant analysis of the Illumina Infinium HumanMethylation450 BeadChip array. Epigenetics Chromatin. 2013;6(4):1-15. doi: 10.1186/1756-8935-6-4. PubMed PMID: 23452981.
56. Hannum G, Guinney J, Zhao L, Zhang L, Hughes G, Sadda S, et al. Genome-wide methylation profiles reveal quantitative views of human aging rates. Mol Cell. 2013;49(2):359-367. doi: 10.1016/j.molcel.2012.10.016. PubMed PMID: 23177740.
57. Laird CD, Pleasant ND, Clark AD, Sneeden JL, Hassan KM, Manley NC, et al. Hairpin-bisulfite PCR: assessing epigenetic methylation patterns on complementary strands of individual DNA molecules. Proc Natl Acad Sci U S A. 2004;101(1):204-209. doi: 10.1073/pnas.2536758100. PubMed PMID: 14673087.
58. Chen ZX, Riggs AD. DNA methylation and demethylation in mammals. J Biol Chem.

2011;286(21):18347-18353. doi: 10.1074/jbc.R110.205286. PubMed PMID: 21454628.

59. Wu SC, Zhang Y. Active DNA demethylation: many roads lead to Rome. Nat Rev Mol Cell Biol. 2010;11(9):607-620. doi: 10.1038/nrm2950. PubMed PMID: 20683471.

60. Weber AR, Krawczyk C, Robertson AB, Kusnierczyk A, Vagbo CB, Schuermann D, et al. Biochemical reconstitution of TET1-TDG-BER-dependent active DNA demethylation reveals a highly coordinated mechanism. Nat Commun. 2016;7(10806):1-13. doi: 10.1038/ncomms10806. PubMed PMID: 26932196.

61. Pastor WA, Aravind L, Rao A. TETonic shift: biological roles of TET proteins in DNA demethylation and transcription. Nat Rev Mol Cell Biol. 2013;14(6):341-356. doi: 10.1038/nrm3589. PubMed PMID: 23698584.

62. Truong TP, Sakata-Yanagimoto M, Yamada M, Nagae G, Enami T, Nakamoto-Matsubara R, et al. Age-Dependent Decrease of DNA Hydroxymethylation in Human T Cells. J Clin Exp Hematop. 2015;55(1):1-6. doi: 10.3960/jslrt.55.1. PubMed PMID: 26105999.

63. Wiehle L, Raddatz G, Musch T, Dawlaty MM, Jaenisch R, Lyko F, et al. Tet1 and Tet2 Protect DNA Methylation Canyons against Hypermethylation. Mol Cell Biol. 2015;36(3):452-461. doi: 10.1128/mcb.00587-15. PubMed PMID: 26598602.

64. Jones PA. Functions of DNA methylation: islands, start sites, gene bodies and beyond. Nat Rev Genet. 2012;13(7):484-492. doi: 10.1038/nrg3230. PubMed PMID: 22641018.

65. Cruickshanks HA, McBryan T, Nelson DM, Vanderkraats ND, Shah PP, van Tuyn J, et al. Senescent cells harbour features of the cancer epigenome. Nat Cell Biol. 2013;15(12):1495-1506. doi: 10.1038/ncb2879. PubMed PMID: 24270890.

66. Schellenberg A, Lin Q, Schuler H, Koch CM, Joussen S, Denecke B, et al. Replicative senescence of mesenchymal stem cells causes DNA-methylation changes which correlate with repressive histone marks. Aging (Albany NY). 2011;3(9):873-888. PubMed PMID: 22025769.

67. Rao X, Evans J, Chae H, Pilrose J, Kim S, Yan P, et al. CpG island shore methylation regulates caveolin-1 expression in breast cancer. Oncogene. 2013;32(38):4519-4528. doi: 10.1038/onc.2012.474. PubMed PMID: 23128390.

68. Kim MS, Kondo T, Takada I, Youn MY, Yamamoto Y, Takahashi S, et al. DNA demethylation in hormone-induced transcriptional derepression. Nature. 2009;461(7266):1007-1012. doi: 10.1038/nature08456. PubMed PMID: 19829383.

69. Oliveira NF, Damm GR, Andia DC, Salmon C, Nociti FH, Jr., Line SR, et al. DNA methylation status of the IL8 gene promoter in oral cells of smokers and non-smokers with chronic periodontitis. J Clin Periodontol. 2009;36(9):719-725. doi: 10.1111/j.1600-051X.2009.01446.x. PubMed PMID: 19659670.

70. Rusiecki JA, Byrne C, Galdzicki Z, Srikantan V, Chen L, Poulin M, et al. PTSD and DNA

Methylation in Select Immune Function Gene Promoter Regions: A Repeated Measures Case-Control Study of U.S. Military Service Members. Front Psychiatry. 2013;4:1-12. doi: 10.3389/fpsyt.2013.00056. PubMed PMID: 23805108.

71. Ushijima T. Epigenetic field for cancerization. J Biochem Mol Biol. 2007;40(2):142-150. PubMed PMID: 17394762.
72. Leung CS. Endogenous Antigen Presentation of MHC Class II Epitopes through Non-Autophagic Pathways. Front Immunol. 2015;6:464. doi: 10.3389/fimmu.2015.00464. PubMed PMID: 26441969.
73. Zhou L, Chong MM, Littman DR. Plasticity of CD4+ T cell lineage differentiation. Immunity. 2009;30(5):646-655. doi: 10.1016/j.immuni.2009.05.001. PubMed PMID: 19464987.
74. Freund A, Orjalo AV, Desprez PY, Campisi J. Inflammatory networks during cellular senescence: causes and consequences. Trends Mol Med. 2010;16(5):238-246. doi: 10.1016/j.molmed.2010.03.003. PubMed PMID: 20444648.
75. Bettelli E, Korn T, Kuchroo VK. Th17: the third member of the effector T cell trilogy. Curr Opin Immunol. 2007;19(6):652-657. doi: 10.1016/j.coi.2007.07.020. PubMed PMID: 17766098.
76. Wilke CM, Bishop K, Fox D, Zou W. Deciphering the role of Th17 cells in human disease. Trends Immunol. 2011;32(12):603-611. doi: 10.1016/j.it.2011.08.003. PubMed PMID: 21958759.
77. Lee JH, Voo KS, Skalnik DG. Identification and characterization of the DNA binding domain of CpG-binding protein. J Biol Chem. 2001;276(48):44669-44676. doi: 10.1074/jbc.M107179200. PubMed PMID: 11572867.
78. Williams K, Christensen J, Helin K. DNA methylation: TET proteins-guardians of CpG islands? EMBO Rep. 2012;13(1):28-35. doi: 10.1038/embor.2011.233. PubMed PMID: 22157888.
79. Ichiyama K, Chen T, Wang X, Yan X, Kim BS, Tanaka S, et al. The methylcytosine dioxygenase Tet2 promotes DNA demethylation and activation of cytokine gene expression in T cells. Immunity. 2015;42(4):613-626. doi: 10.1016/j.immuni.2015.03.005. PubMed PMID: 25862091.
80. Banko JL, Poulin F, Hou L, DeMaria CT, Sonenberg N, Klann E. The translation repressor 4E-BP2 is critical for eIF4F complex formation, synaptic plasticity, and memory in the hippocampus. J Neurosci. 2005;25(42):9581-9590. doi: 10.1523/jneurosci.2423-05.2005. PubMed PMID: 16237163.
81. van der Horst GT, Muijtjens M, Kobayashi K, Takano R, Kanno S, Takao M, et al. Mammalian Cry1 and Cry2 are essential for maintenance of circadian rhythms. Nature.

1999;398(6728):627-630. doi: 10.1038/19323. PubMed PMID: 10217146.

82. Rose-John S, Heinrich PC. Soluble receptors for cytokines and growth factors: generation and biological function. Biochem J. 1994;300:281-290. PubMed PMID: 8002928.

83. Baumann H, Schendel P. Interleukin-11 regulates the hepatic expression of the same plasma protein genes as interleukin-6. J Biol Chem. 1991;266(30):20424-20427. PubMed PMID: 1718962.

84. Heinrich PC, Behrmann I, Haan S, Hermanns HM, Muller-Newen G, Schaper F. Principles of interleukin (IL)-6-type cytokine signalling and its regulation. Biochem J. 2003;374(Pt 1):1-20. doi: 10.1042/bj20030407. PubMed PMID: 12773095.

85. Pflanz S, Hibbert L, Mattson J, Rosales R, Vaisberg E, Bazan JF, et al. WSX-1 and glycoprotein 130 constitute a signal-transducing receptor for IL-27. J Immunol. 2004;172(4):2225-2231. PubMed PMID: 14764690.

86. Vilborg A, Glahder JA, Wilhelm MT, Bersani C, Corcoran M, Mahmoudi S, et al. The p53 target Wig-1 regulates p53 mRNA stability through an AU-rich element. Proc Natl Acad Sci U S A. 2009;106(37):15756-15761. doi: 10.1073/pnas.0900862106. PubMed PMID: 19805223.

87. Vousden KH. Outcomes of p53 activation--spoilt for choice. J Cell Sci. 2006;119(Pt 24):5015-5020. doi: 10.1242/jcs.03293. PubMed PMID: 17158908.

88. Disayabutr S, Kim EK, Cha SI, Green G, Naikawadi RP, Jones KD, et al. miR-34 miRNAs Regulate Cellular Senescence in Type II Alveolar Epithelial Cells of Patients with Idiopathic Pulmonary Fibrosis. PLoS One. 2016;11(6):e0158367. doi: 10.1371/journal.pone.0158367. PubMed PMID: 27362652.

89. Harries LW. MicroRNAs as Mediators of the Ageing Process. Genes (Basel). 2014;5(3):656-670. doi: 10.3390/genes5030656. PubMed PMID: 25140888.

Appendix

S1 Table. GO terms for up- or down-regulated genes in three types of senescent cells.

	Up-regulated genes					
Senescent type	Replicative		RIS		SVts8	
Number of genes	1202		926		1684	
Ranking	Representative GO terms	Enrichment scores	Representative GO terms	Enrichment scores	Representative GO terms	Enrichment scores
1	Developmental process	9.77	Developmental process	8.03	Immune response	7.76
2	Locomotion, Taxis	4.58	Inflammatory response	4.35	Inflammatory response	6.75
3	Inflammatory response	4.08	Angiogenesis	3.45	Regulation of cell migration	4.63
4	Cell migration	3.89	Cell migration	3.31	Locomotion, taxis	4.62
5	Cell adhesion	3.58	Locomotion	3.31	Developmental process	4.61
6	Response to hormone stimulus	3.33	Cell development, Neurogenesis	3.14	Positive/negative regulation of cell death	4.31
7	Regulation of cell migration	3.29	Epidermal cell differentiation, Keratinization	3.04	Regulation of immune response	4.25
8	Muscle contraction	3.16	Wound healing, Blood coagulation	2.79	Cell migration	3.87
9	Blood vessel development	2.76	Regulation of angiogenesis	2.79	Regulation of inflammatory response	3.75
10	Regulation of angiogenesis	2.73	Tissue remodeling	2.28	Regulation of cell differentiation	3.62

*More than 1.3 of enrichment scores gave less than 0.05 p-values.

	Down-regulated genes					
Senescent type	Replicative		RIS		SVts8	
Number of genes	1629		1220		923	
Ranking	Representative GO terms	Enrichment scores	Representative GO terms	Enrichment scores	Representative GO terms	Enrichment scores
1	Cell cycle	36.59	Cell cycle	7.71	Chromatin assembly, Cellular component assembly	11.85
2	Spindle organization, microtubule cytoskeleton organization	10.67	Developmental process	6.72	RNA processing	7.57
3	Chromosome segregation	9.79	Organ development	4.26	Cell cycle process	7.4
4	DNA repair	9.75	Skeletal system development	4.02	Chromosome segregation	3.3
5	M phase of meiotic cell cycle	9.39	Chromosome segregation	3.69	Microtubule cytoskeleton organization	1.76
6	Interphase of mitotic cell cycle	5.25	Positive regulation of cellular component organization	3.6	Amino acid transport	1.63
7	Chromatin assembly	3.9	Bone development	3.4	Regulation of cell cycle	1.45
8	Spindle assembly, Centrosome cycle	3.71	Microtubule cytoskeleton organization	2.99	Negative regulation of RNA metabolic process	1.38
9	DNA unwinding during replication	3.57	Respiratory system development	2.68	Positive/negative regulation of ligase activity	1.36
10	DNA recombination	3.36	Cell adhesion	2.51	Histone methylation	1.14

*More than 1.3 of enrichment scores gave less than 0.05 p-values.

S2 Table. GO terms for hypo- or hyper-methylated genes in replicatively senescent cells.

Rank	Genes with hypomethylation		Genes with hypermethylation	
	GO term categories	Enrichment score	GO term categories	Enrichment score
1	Immune response	7.86	Regulation of biological process	4.24
2	Defense response	3.53	Developmental process	3.85
3	Regulation of immune response	3.02	Regulation of transmission of nerve impulse	3.03
4	Regulation of immune response	2.91	Regionalization	2.42
5	Defense response	2.88	Regulation of secretion, Regulation of localization	1.98
6	Anion transport	2.76	Regulation of respiratory system process	1.92
7	Transport	2.67	Cell communication, Synaptic transmission	1.79
8	Cellular homeostasis	1.96	Cell differentiation	1.75
9	Metal ion transport	1.77	Embryonic limb morphogenesis	1.74
10	Locomotion	1.35	Negative regulation of cell death	1.72

*More than 1.3 of enrichment scores gave less than 0.05 p-values.

S3 Table. The number of genes hosting differentially methylated CpG sites in the gene feature- and the CpG site- subcategories.

Location	Total number of analysis genes		Immune response		Metabolic process		Transport		Cell adhesion		Development		Signal transduction		Transcription		Others	
	Hypo	Hyper	Hypo	Hyper	Hypo	Hyper	Hypo	Hyper	Hypo	Hyper	Hypo	Hyper	Hypo	Hyper	Hypo	Hyper	Hypo	Hyper
TSS1500	1375	4925	160	12	40	879	85	500	67	185	135	682	308	646	0	462	580	1559
TSS200	435	1363	63	0	7	135	76	143	0	17	28	236	54	246	0	61	207	525
5'UTR	769	3003	92	73	16	520	46	238	0	112	158	442	154	418	0	292	303	908
1st exon	476	1189	49	10	0	48	62	133	24	73	0	259	106	220	0	0	235	446
Gene body	3581	7905	209	135	236	1466	456	732	179	347	523	1162	638	1103	33	655	1307	2305
3'UTR	774	909	70	0	44	161	88	0	33	0	109	155	157	157	0	115	273	321
N_Shelf	375	620	0	0	11	104	43	73	31	0	95	99	53	91	0	57	142	196
N_Shore	521	3676	0	103	0	792	54	72	47	147	137	541	86	495	6	407	191	1119
Island	218	4516	0	0	28	618	31	366	0	197	35	745	29	701	24	443	71	1446
S_Shore	509	2929	0	0	0	497	82	315	29	0	96	431	0	406	0	297	302	983
S_Shelf	336	349	0	0	32	27	23	18	28	10	86	39	38	74	0	21	129	160
Open Sea	3713	4809	308	88	400	849	400	459	188	233	472	729	705	690	32	308	1208	1453

S4 Table. Integrated analysis of gene expression and methylation changes in replicatively senescent cells.

Refer to http://rep.toho-u.ac.jp/modules/xoonips/detail.php?id=17120843

S5 Table. Hypo- or hyper-methylated miRNAs in the promoter regions of replicatively senescent cells.

A) Hypomethylated miRNAs

Delta_beta	UCSC RefGene name	UCSC RefGene accession	Chr
-0.47	MIR1912;HTR2C	NR_031733;NM_000868	X
-0.47	MIR548A2	NR_030317	3
-0.44	MIR603;KIAA1217;KIAA1217;KIAA1217	NR_030334;NM_019590;NM_001098500;NM_001098501	10
-0.43	GABRE;MIR452	NM_004961;NR_029973	X
-0.42	GABRE;MIR452	NM_004961;NR_029973	X
-0.42	GABRE;MIR452	NM_004961;NR_029973	X
-0.41	MIR548H3	NR_031679	6
-0.41	MIR548A2	NR_030317	3
-0.39	MIR548A2	NR_030317	3
-0.37	MIR548Q	NR_031752	9
-0.36	C22orf9;C22orf9;MIR1249	NM_001009880;NM_015264;NR_031651	22
-0.35	MIR572	NR_030298	4
-0.35	MIR670	NR_031577	11
-0.35	MIR20B;MIR363;MIR106A;MIR18B;MIR19B2;MIR92A2	NR_029950;NR_029852;NR_029523;NR_029949;NR_029491;NR_029509	X
-0.35	MIR548F3;CNTNAP2	NR_031644;NM_014141	7
-0.33	MIR572	NR_030298	4
-0.33	MIR551B;C3orf50	NR_030294;NR_021485	3
-0.33	MIR128-2;ARPP-21	NR_029824;NM_016300	3
-0.32	MIR453	NR_029969	14
-0.31	MIR1295;FMO3;FMO3	NR_031627;NM_001002294;NM_006894	1
-0.31	MIR888;MIR890	NR_030592;NR_030589	X
-0.30	C22orf9;C22orf9;MIR1249	NM_001009880;NM_015264;NR_031651	22
-0.30	MIR548F3;CNTNAP2	NR_031644;NM_014141	7
-0.30	MIR20B;MIR363;MIR18B;MIR106A;MIR19B2;MIR92A2	NR_029950;NR_029852;NR_029949;NR_029523;NR_029491;NR_029509	X
-0.29	MIR223	NR_029637	X
-0.29	MIR548G	NR_031662	3
-0.29	MIR1275	NR_031681	6
-0.29	MIR135A2	NR_029678	12
-0.29	MIR488;ASTN1;ASTN1	NR_030163;NM_207108;NM_004319	1
-0.29	FAM184A;FAM184A;MIR548B	NM_001100411;NM_024581;NR_030315	6
-0.29	C22orf9;C22orf9;MIR1249	NM_001009880;NM_015264;NR_031651	22
-0.29	C22orf9;C22orf9;MIR1249	NM_001009880;NM_015264;NR_031651	22
-0.28	C22orf9;C22orf9;MIR1249	NM_001009880;NM_015264;NR_031651	22
-0.28	MIR657;AATK	NR_030394;NM_001080395	17
-0.27	MIR526A1	NR_030197	19
-0.27	MIR453;MIR485	NR_029969;NR_030160	14
-0.27	MIR548A2	NR_030317	3
-0.27	C22orf9;C22orf9;MIR1249	NM_001009880;NM_015264;NR_031651	22
-0.27	GABRA3;MIR105-1	NM_000808;NR_029521	X
-0.27	MIR29B1	NR_029517	7
-0.27	RMST;MIR1251	NR_024037;NR_031653	12
-0.26	MIR133B	NR_029903	6
-0.26	CSMD3;MIR2053;CSMD3;CSMD3	NM_198124;NR_031745;NM_052900;NM_198123	8
-0.26	MIR211;TRPM1	NR_029624;NM_002420	15
-0.25	MIR548Q	NR_031752	9
-0.25	VGLL1;MIR934	NM_016267;NR_030631	X
-0.25	VGLL1;MIR934	NM_016267;NR_030631	X
-0.25	DAB1;MIR548D2	NM_021080;NR_030385	1
-0.25	MIR449B;MIR449A;CDC20B;CDC20B;CDC20B	NR_030387;NR_029960;NM_001145734;NM_152623;NM_001170402	5
-0.25	MIR10A	NR_029608	17
-0.25	SLIT3;MIR585	NM_003062;NR_030311	5
-0.25	KIF5C;MIR1978	NM_004522;NR_031742	2
-0.25	MIR489;CALCR;MIR653;CALCR;CALCR	NR_030164;NM_001742;NR_030388;NM_001164737;NM_001164738	7
-0.25	DAB1;MIR548D2	NM_021080;NR_030385	1
-0.24	MIR548F5;NBEA	NR_031646;NM_015678	13
-0.24	ATP2B2;MIR885;ATP2B2	NM_001683;NR_030614;NM_001001331	3
-0.24	MIR548F3;CNTNAP2	NR_031644;NM_014141	7
-0.24	MIR548H4;NOX5;SPESP1	NR_031680;NM_024505;NM_145658	15
-0.24	MIR129-1	NR_029596	7
-0.24	SLIT3;MIR218-2	NM_003062;NR_029632	5
-0.23	MIR128-2;ARPP-21	NR_029824;NM_016300	3
-0.23	MIR1208	NR_031613	8
-0.23	MIR199A1;DNM2;DNM2;DNM2;DNM2	NR_029586;NM_004945;NM_001005361;NM_001005362;NM_001005360	19
-0.23	MIR10A	NR_029608	17
-0.23	MIR199A1;DNM2;DNM2;DNM2;DNM2	NR_029586;NM_004945;NM_001005361;NM_001005362;NM_001005360	19
-0.22	MIR489;CALCR;CALCR;CALCR	NR_030164;NM_001742;NM_001164737;NM_001164738	7
-0.22	MIR892A;MIR892B	NR_030584;NR_030593	X
-0.22	DAB1;MIR548D2	NM_021080;NR_030385	1
-0.22	MIR548I2	NR_031688	4
-0.22	MIR670	NR_031577	11
-0.22	MIR10A	NR_029608	17
-0.22	MIR488;ASTN1;ASTN1	NR_030163;NM_207108;NM_004319	1
-0.22	MIR146B	NR_030169	10
-0.22	TTN;TTN;TTN;MIR548N;TTN	NM_133378;NM_133432;NM_003319;NR_031666;NM_133437	2
-0.22	MIR147	NR_029604	9
-0.22	MIR516B1	NR_030212	19
-0.22	MIR206	NR_029713	6
-0.22	RMST;MIR1251	NR_024037;NR_031653	12
-0.21	MIR548F3;CNTNAP2	NR_031644;NM_014141	7
-0.21	MIR320B1	NR_031564	1
-0.21	MIR891B	NR_030590	X
-0.21	MIR520A	NR_030189	19
-0.21	MIR516A2	NR_030221	19
-0.21	MIR135A2	NR_029678	12
-0.21	MIR524	NR_030200	19
-0.21	HTR2C;MIR1298	NM_000868;NR_031578	X
-0.21	MIR609;C10orf79	NR_030340;NM_025145	10
-0.21	MIR921;FAM78B	NR_030626;NM_001017961	1
-0.21	RBPMS2;MIR1272	NM_194272;NR_031674	15
-0.21	MIR516A2	NR_030221	19
-0.20	MIR519E	NR_030185	19
-0.20	GABRA3;MIR767;MIR105-1	NM_000808;NR_030409;NR_029521	X
-0.20	MIR1323	NR_031568	19
-0.20	MIR548H4	NR_031680	15
-0.20	MIR128-2;ARPP-21	NR_029824;NM_016300	3
-0.20	MIR506	NR_030233	X
-0.20	MIR23A;MIR27A;MIR24-2	NR_029495;NR_029501;NR_029497	19
-0.20	MIR891A	NR_030581	X

B) Hypermethylated miRNAs

Delta_beta	UCSC RefGene name	UCSC RefGene accession	Chr
0.62	MGC16121;MIR503	NR_024607;NR_030228	X
0.60	MGC16121;MIR503	NR_024607;NR_030228	X
0.52	MIR193A	NR_029710	17
0.48	MIR193A	NR_029710	17
0.48	MAB21L1;MIR548F5;NBEA	NM_005584;NR_031646;NM_015678	13
0.45	SNORD12B;C20orf199;MIR1259;C20orf199;SNORD12;ZNFX1;C20orf19	NR_003695;NR_003605;NR_031660;NR_003606;NR_003030;NM_021035;NR_003604	20
0.43	MIR193A	NR_029710	17
0.43	MGC16121;MIR503	NR_024607;NR_030228	X
0.40	C3orf26;FILIP1L;MIR548G;FILIP1L	NM_032359;NM_182909;NR_031662;NM_001042459	3
0.38	MAB21L1;MIR548F5;NBEA	NM_005584;NR_031646;NM_015678	13
0.38	MAB21L1;MIR548F5;NBEA	NM_005584;NR_031646;NM_015678	13
0.36	MIR7-2	NR_029606	15
0.35	MAB21L1;MIR548F5;NBEA	NM_005584;NR_031646;NM_015678	13
0.35	MGC16121;MIR503	NR_024607;NR_030228	X
0.33	MIR193A	NR_029710	17
0.33	MIR377	NR_029869	14
0.33	CACNG8;MIR935	NM_031895;NR_030632	19
0.33	MIR375	NR_029867	2
0.32	MGC16121;MIR503	NR_024607;NR_030228	X
0.32	MIR564;TMEM42	NR_030290;NM_144638	3
0.32	MIR548Q;ZNF462	NR_031752;NM_021224	9
0.32	MIR548H4;SPESP1;NOX5	NR_031680;NM_145658;NM_024505	15
0.31	MIR148B;COPZ1	NR_029894;NM_016057	12
0.31	MIR375	NR_029867	2
0.31	RDBP;SKIV2L;MIR1236	NM_002904;NM_006929;NR_031601	6
0.31	MCM7;MCM7;MIR25	NM_005916;NM_182776;NR_029498	7
0.30	MIR141;MIR200C	NR_029682;NR_029779	12
0.30	MIR505	NR_030230	X
0.30	NCRNA00164;MIR663B	NR_027020;NR_031608	2
0.30	MIR596	NR_030326	8
0.29	MIR375	NR_029867	2
0.29	CACNG8;MIR935	NM_031895;NR_030632	19
0.29	MIR7-2	NR_029606	15
0.28	MIR548H4;NOX5	NR_031680;NM_024505	15
0.28	MIR663	NR_030386	20
0.28	MIR346;GRID1	NR_029907;NM_017551	10
0.28	MIR874;KLHL3	NR_030588;NM_017415	5
0.28	MIR548F5;NBEA	NR_031646;NM_015678	13
0.28	MIR1306;DGCR8	NR_031706;NM_022720	22
0.28	MIR657;AATK;MIR338	NR_030394;NM_001080395;NR_029897	17
0.27	MIR612	NR_030343	11
0.27	VWA5B2;MIR1224	NM_138345;NR_030410	3
0.27	MIR202	NR_030170	10
0.27	PRG4;PRG4;PRG4;PRG4;MIR548F1	NM_005807;NM_001127710;NM_001127708;NM_001127709;NR_031642	1
0.26	FOXP1;MIR1284;FOXP1	NM_032682;NR_031697;NM_001012505	3
0.26	CCPG1;MIR628;CCPG1	NM_020739;NR_030358;NM_004748	15
0.25	C3orf52;MIR567	NM_024616;NR_030292	3
0.25	MIR548H4;NOX5;NOX5;SPESP1;SPESP1	NR_031680;NM_024505;NM_024505;NM_145658;NM_145658	15
0.25	MGC16121;MIR424;MIR503	NR_024607;NR_029946;NR_030228	X
0.25	MIR130A	NR_029673	11
0.25	MIR17HG;MIR17HG	NR_027349;NR_027350	13
0.25	MIR212	NR_029625	17
0.25	MIR149;PP14571;GPC1	NR_029702;NR_024014;NM_002081	2
0.25	MIR130B;MIR301B	NR_029845;NR_030622	22
0.24	MIR212	NR_029625	17
0.24	MIR149;PP14571;GPC1	NR_029702;NR_024014;NM_002081	2
0.24	C3orf26;FILIP1L;MIR548G;FILIP1L	NM_032359;NM_182909;NR_031662;NM_001042459	3
0.24	MYH7B;MIR499	NM_020884;NR_030223	20
0.24	MIR196A1	NR_029582	17
0.24	MIR505	NR_030230	X
0.24	MIR2110;C10orf118	NR_031747;NM_018017	10
0.24	MIR663	NR_030386	20
0.24	CTDSP1;MIR26B;CTDSP1	NM_182642;NR_029500;NM_021198	2
0.24	CTDSP1;MIR26B;CTDSP1	NM_182642;NR_029500;NM_021198	2
0.23	MIR196B	NR_029911	7
0.23	RDBP;SKIV2L;MIR1236	NM_002904;NM_006929;NR_031601	6
0.23	MIR2110;C10orf118	NR_031747;NM_018017	10
0.23	MIR503;MGC16121	NR_030228;NR_024607	X
0.23	MEST;MIR335;MEST;MEST	NM_177524;NR_029899;NM_177525;NM_002402	7
0.23	MIR1915;C10orf114	NR_031736;NM_001010911	10
0.23	CACNG8;MIR935	NM_031895;NR_030632	19
0.23	MIR548H4;NOX5	NR_031680;NM_024505	15
0.22	MIR1207;PVT1	NR_031612;NR_003367	8
0.22	PTPRN;MIR153-1	NM_002846;NR_029688	2
0.22	MIR424;MGC16121;MIR503	NR_029946;NR_024607;NR_030228	X
0.22	MIR548N	NR_031666	2
0.22	MIR219-2	NR_029837	9
0.22	MIR802	NR_030414	21
0.22	MIR1470;WIZ	NR_031716;NM_021241	19
0.22	MIR219-1	NR_029633	6
0.22	MIR548Q	NR_031752	9
0.22	MIR629;TLE3;TLE3;TLE3	NR_030714;NM_001105192;NM_020908;NM_005078	15
0.22	MIR30E;NFYC;NFYC;NFYC;NFYC;NFYC	NR_029846;NM_001142589;NM_014223;NM_001142587;NM_001142588;NM_00114259	1
0.21	MIR138-1	NR_029700	3
0.21	MAB21L1;MIR548F5;NBEA	NM_005584;NR_031646;NM_015678	13
0.21	MIR148B;COPZ1	NR_029894;NM_016057	12
0.21	CACNG8;MIR935	NM_031895;NR_030632	19
0.21	MIR614	NR_030345	12
0.21	MIR196B	NR_029911	7
0.21	MIR216B	NR_030623	2
0.21	MIR589;FBXL18	NR_030318;NM_024963	7
0.21	MIR150	NR_029703	19
0.21	MIR141;MIR200C	NR_029682;NR_029779	12
0.20	PKD1;MIR1225;PKD1	NM_001009944;NR_030646;NM_000296	16
0.20	MIR149;PP14571;GPC1	NR_029702;NR_024014;NM_002081	2
0.20	MAB21L1;MIR548F5;NBEA;MAB21L1	NM_005584;NR_031646;NM_015678;NM_005584	13
0.20	PKD1;MIR1225;PKD1	NM_001009944;NR_030646;NM_000296	16
0.20	LYST;MIR1537	NM_000081;NR_031718	1
0.20	MIR130B	NR_029845	22
0.20	MIR345;SLC25A29	NR_029906;NM_001039355	14
0.20	MIR375	NR_029867	2
0.20	MIR9-3	NR_029692	15

S6 Table. miRNA expression regulated by DNA methylation in the promoter region.

Hypermethylation & down-regulated expression				
Seq.	miRNA	Methylation (Δß)	Expression (fold-change)	
		PDL 85 VS PDL 36	PDL 78 VS PDL 44	PDL 80 VS PDL 44
1	hsa-miR-193a-5p	0.4	-1.5	-1.7
2	hsa-miR-7-5p	0.3	-1.7	-2.3
3	hsa-miR-25-3p	0.3	-1.9	-2.4
4	hsa-miR-505-3p	0.3	-2.0	-1.8
5	hsa-miR-17-5p	0.2	-1.6	-2.1
6	hsa-miR-335-5p	0.2	-1.4	-1.9
7	hsa-miR-130b-3p	0.2	-1.6	-2.1

* If miRNA had several probes, Δß was the mean of hypermethylated probes.

* miRNA with hypomethylation and expression increase was not detected.

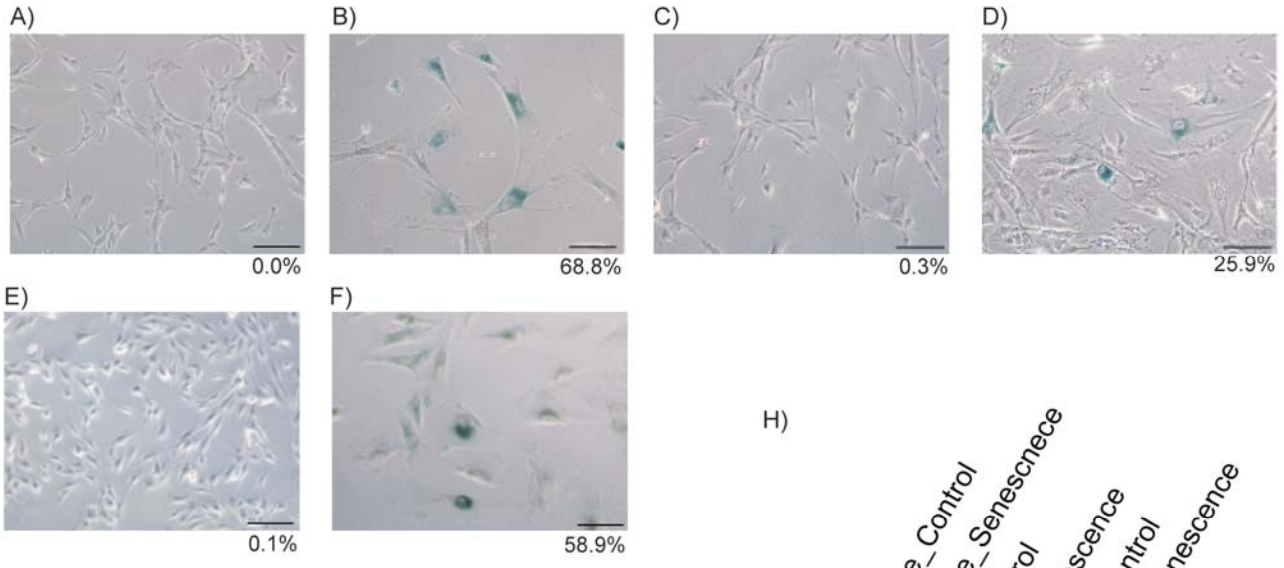

G)

		Microarray	qRT-PCR
		Foldchange	Foldchange
p16	Replicative	5.8	2.7
	Ras	5.4	5.3
	SVts8	1.1	0.9
p21	Replicative	8.7	2.5
	Ras	2.5	2.0
	SVts8	36.4	30.1

S1 Fig. Confirmation of senescence.

Senescent cells were subjected to senescence-associated beta-galactosidase (SA-ß-Gal) staining, qRT-PCR and immunoblotting. SA-ß-Gal staining of the control A), C), E), replicatively senescent B), RIS D), and senescent SVts8 cells F). The percentages of SA-ß-Gal-positive cells are shown at the bottom of each picture. Bar, 200 μm. Objective, ×10. G) The expression levels of $p16^{INK4A}$ and $p21^{Cip1/Waf1}$ obtained with SurePrint G3 Human GE microarrays and qRT-PCR. H) Representative western blotting of $p16^{INK4A}$ and $p21^{Cip1/Waf1}$, Ras, and loading control (actin). Images of $p16^{INK4A}$ are shown separately shown due to different exposure time.

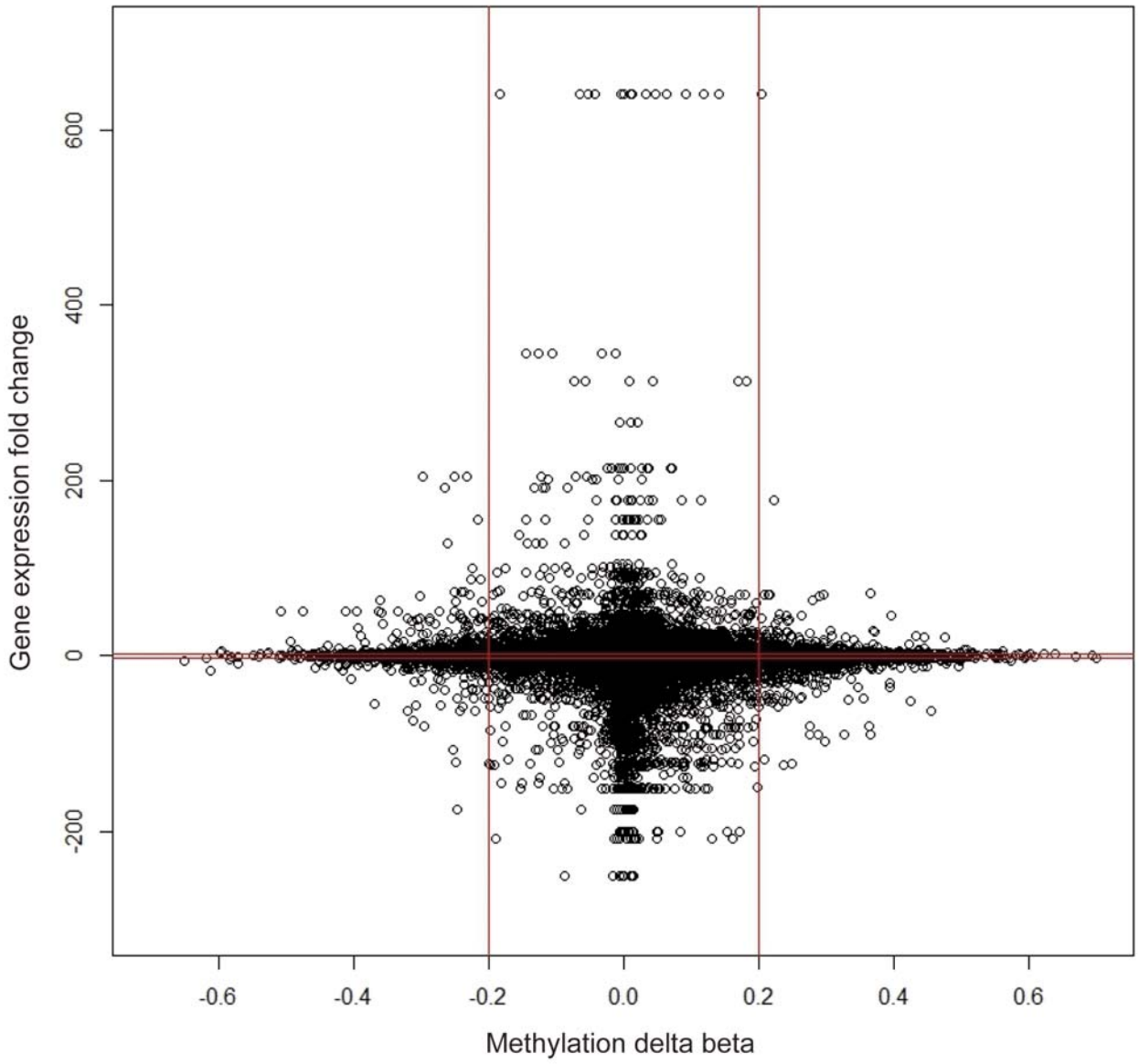

S2 Fig. Integrated analysis of methylation and gene expression in replicative senescence.

Each plot represents the values obtained from a single gene using integrated analyses. DNA methylation ß values and gene expression levels are plotted along the abscissa and the ordinate, respectively. Red lines show the cut-off border. For methylation, Δß for hypermethylation is >= 0.2, Δß for hypomethylation is =< −0.2. For gene expression, the cut-off for increased/decreased expression was a ±2-fold change.